CrystEngComm

Accepted Manuscript

This article can be cited before page numbers have been issued, to do this please use: R. shukla, A. Saeed, J. Simpson and D. Chopra, *CrystEngComm*, 2017, DOI: 10.1039/C7CE01310H.

ROYAL SOCIETY OF CHEMISTRY

rsc.li/crystengcomm

View Article Online
DOI: 10.1039/C7CE01310H

Quantitative investigation of C-H···π and other intermolecular interactions in a series of crystalline N-(substituted phenyl)-2-naphthamide derivatives.

Rahul Shukla[a], *Aamer Saeed*[*b], *Jim Simpson*[*c] *and Deepak Chopra*[*a]
[a] *Crystallography and Crystal Chemistry Laboratory, Department of Chemistry, IISER Bhopal, Bhopal 462066, Madhya Pradesh, India.*
E-mail: dchopra@iiserb.ac.in; Tel: +91 0755 669 1311
[b] *Department of Chemistry, Quaid-i-Azam University-45320, Islamabad, Pakistan*
E-mail aamersaeed@yahoo.com Fax +9251 9064 2241; Tel +9251 9064 2128
[c] *Department of Chemistry, University of Otago, P.O. Box 56, Dunedin 9054, New Zealand*
E-mail: jsimpson@alkali.otago.ac.nz; Fax +643 479 7906; Tel: +643 479 7914

Abstract

In this study, we have investigated the nature and characteristics of different intermolecular interactions present in a series of seven N-(substituted phenyl)-2-naphthamides. The seven structures comprise 2-naphthyl ring systems linked by amide bridges to N-bound phenyl, **1**, or substituted benzene rings **3**-**7**, or in the case of **2**, a cyclohexane ring. A common feature of the crystal packing for all but the *o*-nitro derivative **7** is the presence of a strong intermolecular N-H···O interaction. In case of **7**, the possibility of such an interaction is obviated by the formation of an intramolecular N-H···O hydrogen bond. An additional feature of the crystal packing for **1**—**6** is the significant roles that C—H···π contacts play in generating three dimensional networks. In contrast for **7**, the intramolecular N—H···O hydrogen bond precludes the formation of molecular chains but the planar nature of this molecule allows significant π···π stacking interactions to stabilize the packing.

Introduction

Understanding the role of intermolecular interaction and their contribution to molecular packing is one of the very important aspects of crystal engineering.[1-5] Intermolecular interactions also play very important roles in both chemistry[6-9] and biology.[10-13] The fact that intermolecular interactions can be used very efficiently to design new materials with desirable properties[14-16] has attracted immense attention from the scientific community. Hydrogen bonds are one of the most studied intermolecular interactions. These are defined as "an attractive interaction between a hydrogen atom from a molecule or a molecular fragment X–H in which X is more electronegative than H, and an atom or a group of atoms in the same or a different molecule, in which there is evidence of bond formation".[17-18] While strong hydrogen bonds such as N/O-H···O/N[19-20] are well recognized and characterized, the focus in the past decade has shifted to investigations of role of weak hydrogen bonds such as such as C-H···X (X = O, N, S, halogens and π-electrons)[21-34] in molecular crystals. Among these weak

View Article Online
DOI: 10.1039/C7CE01310H

hydrogen bonds, C-H···π interactions have garnered significant attention due to their unique features and characteristics. Some consider these contacts to be in the grey area between hydrogen bonds and van der Waals interactions rather than pure hydrogen bonds.[35] Another interesting feature of the C-H···π interaction is that it is mainly dispersive in nature[36-40] as opposed to traditional hydrogen bonds which are largely considered to be electrostatic interactions.[41-42] Regardless of the nature of the contacts, C-H···π interactions have established themselves as important interacting forces because of their role not only in molecular crystals[31,34,43-46] but also in several other areas including chiral recognition[47-48], polymer chemistry,[49-50] coordination chemistry,[51-52] biochemistry,[53-54] and the structures of DNA[55-56] and proteins.[57-58] Several theoretical studies on model complexes have also been performed in order to understand these interactions from a quantitative point of view.[59-60] Therefore, a systematic investigate of the role of attractive C-H···π interactions alongside other intermolecular interactions is desirable.

In this study we have synthesized a series of seven N-substituted 2-naphthamide derivatives. Of the seven derivatives reported here, the 2-napthamide substituents include N-bound phenyl, **1**, cyclohexyl, **2**, and five substituted benzene rings, **3**-**7**. Napathamide derivatives are an important class of compound which exhibit a range of biological functions. These include use in *in vitro* studies,[61] as kinase inhibitors,[62] in the determination of binding affinities,[63] as antipsychotic agents[64] and in the treatment of Alzheimer's disease.[65] In view of these important applications, it is of interest to systematically and quantitatively explore the molecular geometry and intermolecular interactions that are involved in the formation of crystals of this class of molecules. The recent emergence of a variety of computational tools such as PIXEL, XPAC2.0 and Crystal Explorer will assist in the quantitative investigation of C-H···π and other intermolecular interactions present in the crystal structures of the molecules reported here.

Experimental Section

Synthesis of N-(substituted phenyl)-2-naphthamides (**1**—**7**)

The N-(substituted phenyl)-2-naphthamides (**1**-**7**) were synthesized in a single step carbonyldiimidazole promoted process shown in Scheme 1, which was originally developed for the one-pot synthesis of N,N-disubstituted anilines.[66] 2-Naphthoic acid (10 mmol) was added slowly with stirring to a solution of carbonyldiimidazole (CDI) (10 mmol) dissolved in 30 mL dry THF at room temperature under nitrogen atmosphere. The reaction mixture was further stirred for 15 min and a solution of the appropriate aniline (10 mmol) in 30 mL dry THF was added slowly. The

View Article Online
DOI: 10.1039/C7CE01310H

stirring was continued for an additional 10 min at room temperature then the mixture refluxed for 3 h. After completion of the reaction, monitored by TLC, the reaction mixture was concentrated to obtain the crude products in 76—91% yields as white solids. Colourless crystals were obtained in each case on slow evaporation from a methanol solution.

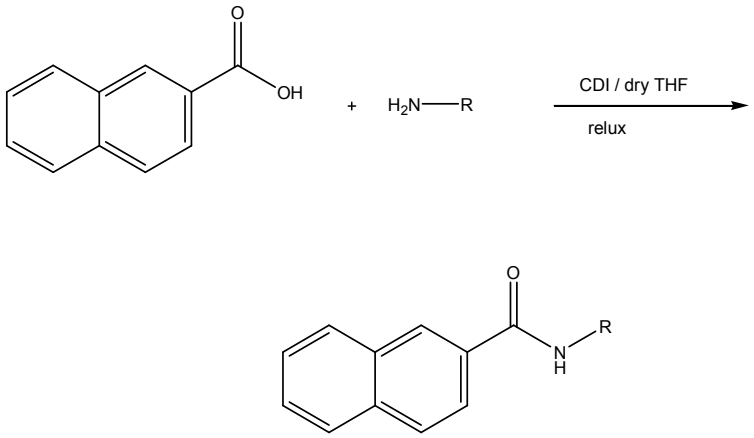

Scheme 1. Synthesis of *N*-phenyl-2-naphthamide derivatives. R = C_6H_5, **1**; C_6H_{11}, **2**; 3-CH_3-C_6H_5, **3**; 4-Cl-C_6H_5, **4**; 3-CH_3O-C_6H_5, **5**; 4-$CH_3OC_6H_5$, **6** and 2-O_2N-C_6H_5, **7**.

N-Phenyl-2-naphthamide, **1**

Yield: 77 %; m.p: 185°C; IR (pure, cm^{-1}): 3262 (N-H), 3066 (Csp^2-H), 1674 (CONH), 1588 (C=C, Ar), ^{1}H-NMR (300MHz, DMSO-d_6): δ 8.51 (s, 1H, NH), 8.22-8.13 (m, 2H, Ar-H), 8.09-8.04 (m, 2H, Ar-H), 7.86-7.83 (m, 1H, Ar-H), 7.75-7.59 (m, 4H, Ar-H), 7.52-7.49 (m, 3H, Ar-H); ^{13}C-NMR (75.4 MHz, DMSO-d6): δ 180.7, 155.92, 133.4, 132.2, 131.5, 129.9, 129.03 127.9, 127.7, 127.0, 126.4, 125.17 119.8; Anal. Calcd. For C_{17} H_{13} N O: C, 82.57; H, 5.30; N, 5.66; Found: C, 82.61; H, 5.29; N, 5.68; GC-MS *m/z*: 247.02, ($M^{\cdot+}$).

N-Cyclohexyl-2-naphthamide, **2**

Yield: 74 %; m.p: 176°C; IR (pure, cm^{-1}): 3271 (N-H), 3060 (Csp^2-H), 2926 (CH_2), 1641 (CONH), 1586 (C=C, Ar), 1641 (CONH), ^{1}H-NMR (300MHz, DMSO-d_6): δ 8.22-8.13 (m, 2H, Ar-H), 8.09-8.04 (m, 2H, Ar-H), 7.86-7.83 (m, 1H, Ar-H), 7.75-7.59 (m, 2H, Ar-H), 1.18-1.45 (4H, m, CH_2 x 2), 1.60-1.76 (4H, m, CH_2 x 2), 1.94-2.02 (2H, dd, CH_2), 3.94 (1H, m, CH); ^{13}C-NMR (75.4 MHz, DMSO-d6): δ 180.7, 133.4, 132.2, 131.5, 129.9, 129.03 127.9, 127.7, 127.0, 126.4, 25.81 (CH_2-4 cycl), 24.75 (CH_2-3), 33.03 (CH_2-2), 53.71 (CH); Anal. Calcd. For C_{17} H_{19} N O: C, 80.60; H, 7.56; N, 5.53; Found: C, 80.56; H, 7.61; N, 5.57; GC-MS *m/z*: 253.15, ($M^{\cdot+}$).

N-(m-Tolyl)-2-naphthamide, 3

Yield: 81 %; m.p: 192°C; IR (pure, cm^{-1}): 3271 (N-H), 3063 (Csp^2-H), 1675 (CONH), 1587 (C=C, Ar), ^{1}H-NMR 300MHz, DMSO-d_6): δ 7.91 (s, 1H, NH), 8.25-8.23 (d, 1H, *J*=8.1 Hz, Ar-H), 8.14 (d, 1H, *J*=8.1 Hz, Ar-H), 8.06-8.01 (m, 2H, Ar-H), 7.88-7.86 (m, 1H, Ar-H), 7.70-7.59 (m, 4H, Ar-H),

View Article Online
DOI: 10.1039/C7CE01310H

7.46 (t, 1H, *J*=8.1 Hz, Ar-H), 2.51 (s, 3H, CH_3); ^{13}C-NMR (75.4 MHz, DMSO-d6): δ 161.9, 138.0, 133.5, 132.4, 132.2, 131.4, 129.9, 129.1, 129.0, 128.3, 128.1, 128.0, 127.8, 127.6, Anal. Calcd. For $C_{18}H_{15}NO$: C, 82.73; H, 5.79; N, 5.36; Found: C, 82.69; H, 5.81; N, 5.37; GC-MS *m/z*: 261.1, ($M^{\cdot+}$).

N-(4-Chlorophenyl)-2-naphthamide, **4**

Yield: 83%; m.p: 179°C; IR (pure, cm^{-1}): 3250 (N-H), 1668 (CO), 1577 (C=C), 780 (C-Cl); ^{1}H-NMR 300MHz, DMSO-d6): δ 8.4 (s, 1H, NH), 8.3 (d, 1H, *J*=7.8, Ar-H), 8.06-8.02 (m, 2H, Ar-H), 7.83-7.79 (m, 3H, Ar-H), 7.68 (d, 2H, *J*=8.4, Ar-H), 7.42 (d, 2H, *J*=8.4, Ar-H); ^{13}C-NMR (75.4 MHz, DMSO-d6): δ 169.3, 170.4, 160.3 137.6, 133.4, 132.0, 131.8, 129.9, 128.9, 127.8, 127.6, 126.9, 125.2; Anal. Calcd. For $C_{17}H_{12}$ ClNO: C, 72.47; H, 4.29; N, 4.97; Found: C, 72.52; H, 4.31; N, 4.93; GC-MS *m/z*: 281.0, 283.0 ($M^{\cdot+}$).

N-(3-Methoxyphenyl)-2-naphthamide, **5**

Yield: 89%; m.p: 181°C; IR (pure, cm^{-1}): 3250 (N-H), 2950 (CH_3), 1668 (CO), 1577 (C=C), 1265 (C=S), ^{1}H-NMR 300MHz, DMSO-d6): δ 8.03 (s, 1H, NH), 8.13 (d, 1H, *J*=8.4, Ar-H), 8.06-8.02 (m, 1H, Ar-H), 7.83-7.79 (m, 2H, Ar-H), 7.68-7.58 (m, 3H, Ar-H), 7.42-7.31 (m, 2H, Ar-H), 4.01 (s, 3H, OCH_3); ^{13}C-NMR (75.4 MHz, DMSO-d6): δ 165.4, 160.3 137.6, 133.4, 132.0, 131.8, 129.9, 128.9, 127.8, 127.6, 126.9, 125.2, 122.7, 56.1 Anal. Calcd. For $C_{18}H_{15}NO_2$: C, 77.96; H, 5.45; N, 4.97; Found: C, 77.91; H, 5.49; N, 5.07; GC-MS *m/z*: 277.2 ($M^{\cdot+}$).

N-(4-Methoxyphenyl)-2-naphthamide, **6**

Yield: 91%; m.p: 201°C; IR (pure, cm^{-1}): 3250 (N-H), 2950 (CH_3), 1668 (CO), 1577 (C=C), 1265 (C=S), ^{1}H-NMR 300MHz, DMSO-d6): δ 8.3 (s, 1H, NH), 7.81 (d, 1H, *J*=7.8, Ar-H), 7.79 (d, 1H, *J*=8.4, Ar-H), 7.83-7.79 (m, 2H, Ar-H), 7.68-7.58 (m, 3H, Ar-H), 7.42-7.31 (m, 2H, Ar-H), 3.97 (s, 3H, Ar-OCH_3); ^{13}C-NMR (75.4 MHz, DMSO-d6): δ 169.5, 170.4, 160.3 137.6, 133.4, 132.0, 131.8, 129.9, 128.9, 127.8, 127.6, 126.9, 125.2, 122.7, 56.2; Anal. Calcd. For $C_{18}H_{15}NO_2$: C, 77.96; H, 5.45; N, 5.05; Found: C, 78.01; H, 5.41; N, 5.09; GC-MS *m/z*: 277.2 ($M^{\cdot+}$).

N-(2-Nitrophenyl)-2-naphthamide, **7**

Yield: 76 %; m.p: 189°C; IR (pure, cm^{-1}): 3271 (N-H), 3063 (Csp^2-H), 1675 (CONH), 1564 (-NO_2), 1587 (C=C), ^{1}H-NMR 300MHz, DMSO-d_6): δ 8.70 (s, 1H, NH), 8.33 (m, 4H, Ar-H), 8.25-8.23 (d, 1H, *J*=8.1 Hz, Ar-H), 8.14 (d, 1H, *J*=8.1 Hz, Ar-H), 8.06-8.01 (m, 2H, Ar-H), 7.88-7.86 (m, 1H, Ar-H), 7.70-7.59 (m, 2H, Ar-H),; ^{13}C-NMR (75.4 MHz, DMSO-d6): δ 164.9, 149.92, 138.0, 133.5, 132.4, 132.2, 131.4, 129.9, 129.1, 129.0, 129.58, 128.3, 128.1, 128.0, 127.8, 127.4. Anal. Calcd. For $C_{17}H_{12}N_2O_3$: C, 69.86; H, 4.14; N, 9.58; Found: C, 69.90; H, 4.11; N, 9.60; GC-MS *m/z*: 298.0 ($M^{\cdot+}$).

X-ray structure determinations

X-ray measurements for **1**—**7** were carried out on a Bruker APEXII Kappa CCD single crystal diffractometer equipped with a graphite monochromator. MoK_α radiation (λ = 0.71073 Å) was used

View Article Online
DOI: 10.1039/C7CE01310H

for all of the collections which were controlled by APEX2[67] with data collected at 89(2) K. Data were corrected for Lorentz and polarization effects using SAINT[67] and multi-scan absorption corrections were applied using SADABS.[67] The structures were solved by direct methods (SHELXS-97)[68] and refined using full-matrix least-squares procedures (SHELXL-97[68] and Titan2000[69]). All non-hydrogen atoms were refined anisotropically and all hydrogen atoms bound to carbon were placed in the calculated positions, and their thermal parameters were refined isotropically with U_{eq} = 1.2—1.5 U_{eq}(C). The N—H hydrogen atoms were located in difference Fourier maps and their coordinates were refined with U_{eq} = 1.2 U_{eq}(N). Compound **5** crystallised with two unique but closely similar molecules, designated A and B, in the unit cell. These overlay with an rms deviation of 0.1105 Å and the numbering scheme labels atoms with a trailing A or B as appropriate. Two reflections for **1**, one for each of **2**, **3**, **4** were found to be clearly affected by the beam-stop and these were omitted from the final refinement. Compounds **1**, **2** and **5** crystallised in non-centric space groups but the absence of a heavy atom meant that the absolute structure could not be reliably determined. Despite this, Friedel opposites were not merged in the final refinement. All molecular plots and packing diagrams were drawn using Mercury[70] and additional metrical data were calculated using PLATON.[71] Tables were prepared using WINGX.[72] Details of the X-ray measurements and crystal data for all of the complexes are given in Table 1.

Table 1 Crystal data and structure refinement of 1-7

	1	**2**	**3**
Empirical formula	$C_{17}H_{13}NO$	$C_{17}H_{19}NO$	$C_{18}H_{15}NO$
Formula weight	247.28	253.33	261.31
Temperature (K)	89(2)	89(2)	89(2)
Wavelength (Å)	0.71073	0.71073	0.71073
Crystal system	Monoclinic	Monoclinic	Monoclinic
Space group	C c	P 2_1	P 2_1/c
a (Å)	28.7372(16)	5.1820(9)	26.362(2)
b (Å)	5.4797(3)	6.5439(11)	5.8842(5)
c (Å)	7.8381(5)	19.416(3)	8.6253(7)
α (°)	90	90	90
β (°)	104.767(3)	92.448(9)	92.291(5)
γ (°)	90	90	90
V (A^3)	1193.51(12)	657.81(19)	1336.9(2)
Z	4	2	4
D_{calc} (gcm^{-3})	1.376	1.279	1.298
μ (mm^{-1})	0.086	0.079	0.080
F (000)	520	272	552
Crystal size	0.52 x 0.42 x 0.04	0.38 x 0.18 x 0.13	0.46 x 0.24 x 0.15
Theta range for data collection	4.32 – 31.99	3.29 – 33.40	2.32 – 33.16

View Article Online
DOI: 10.1039/C7CE01310H

Reflections collected independent observed	10441 3533 [R(int) = 0.0380] 3049	10572 4420 [R(int)= 0.0309] 3873	22348 4687 [R(int)= 0.0545] 3578
Min. and max. transmission	1.0000, 0.7968	1.0000, 0,8339	1.0000, 0.7414
Data/restraints/parameters	3533 / 2 / 175	4420/1/175	4687/0/185
Goodness-of-fit	1.043	1.090	1.084
Final R indices [I >2σ(I)]	R_1 = 0.0445, wR_2 = 0.1103	R_1 = 0.0486, wR_2 = 0.1417	R_1 = 0.0895, wR_2 = 0.2443
R indices (all data)	R_1 = 0.0529, wR_2 = 0.1152	R_1 = 0.0628, wR_2 = 0.1692	R_1 = 0.1086, wR_2 = 0.2550
Largest difference peak and hole (e $Å^{-3}$)	0.409 and -0.231	0.652 and -0.489	0.790 and -0.468
CCDC reference number	997577	997578	997579

View Article Online
DOI: 10.1039/C7CE01310H

	4	**5**	**6**
Empirical formula	$C_{17}H_{12}NOCl$	$C_{18}H_{15}NO_2$	$C_{18}H_{15}NO_2$
Formula weight	281.73	277.31	277.31
Temperature (K)	89(2)	89(2)	89(2)
Wavelength (Å)	0.71073	0.71073	0.71073
Crystal system	Triclinic	Orthorhombic	Triclinic
Space group	P -1	$P\ 2_12_12_1$	P -1
a (Å)	5.5994(11)	9.7762(5)	5.5162(6)
b (Å)	7.4730(15)	11.4779(5)	7.4987(7)
c (Å)	15.867(3)	24.3526(11)	16.1006(17)
α (°)	88.78(3)	90	86.535(3)
β (°)	84.12(3)	90	87.169(4)
γ (°)	84.82(3)	90	86.154(4)
V (A^3)	657.7(2)	2732.6(2)	662.59(12)
Z	2	8	2
D_{calc} (gcm^{-3})	1.423	1.348	1.390
μ (mm^{-1})	0.284	0.088	0.091
F (000)	292	1168	292
Crystal size	0.48 x 0.25 x 0.13	0.66 x 0.30 x 0.19	0.58 x 0.25 x 0.21
Theta range for data collection	3.01 – 33.29	1.67 – 33.44	1.27 – 33.42
Reflections collected independent observed	12246 4495 [R(int) = 0.0306] 3668	51581 9858 [R(int)= 0.0435] 8343	12388 4594 [R(int)= 0.0336] 3658
Min. and max. transmission	1.0000, 0.8373	1.0000, 0.8468	1.0000, 0.8205
Data/restraints/parameters	4495 / 2 / 184	9858/2/387	4594/1/195
Goodness-of-fit	1.065	1.043	1.071
Final R indices [$I > 2\sigma(I)$]	$R_1 = 0.0392$, $wR_2 = 0.1044$	$R_1 = 0.0431$, $wR_2 = 0.1073$	$R_1 = 0.0464$, $wR_2 = 0.1374$
R indices (all data)	$R_1 = 0.0494$, $wR_2 = 0.1104$	$R_1 = 0.0555$, $wR_2 = 0.1144$	$R_1 = 0.0588$, $wR_2 = 0.1534$
Largest difference peak and hole (e $Å^{-3}$)	0.479 and -0.280	0.429 and -0.220	0.578 and -0.363
CCDC reference number	997580	997581	997582

View Article Online
DOI: 10.1039/C7CE01310H

	7
Empirical formula	$C_{17}H_{12}N_2O_3$
Formula weight	292.29
Temperature (K)	89(2)
Wavelength (Å)	0.71073
Crystal system	Triclinic
Space group	P -1
a (Å)	7.2920(6)
b (Å)	8.1868(6)
c (Å)	12.1035(10)
α (°)	86.710(5)
β (°)	84.055(5)
γ (°)	65.201(4)
V (A^3)	652.32(9)
Z	2
D_{calc} (gcm^{-3})	1.488
μ (mm^{-1})	0.104
F (000)	304
Crystal size	0.52 x 0.26 x 0.04
Theta range for data collection	3.73 – 28.83
Reflections collected independent observed	9255 3345 [R(int) = 0.0376] 2362
Min. and max. transmission	1.0000, 0.8726
Data/restraints/parameters	3345 / 0 / 202
Goodness-of-fit	1.037
Final R indices [I >2σ(I)]	R_1 = 0.0505, wR_2 = 0.1174
R indices (all data)	R_1 = 0.0789, wR_2 = 0.1308
Largest difference peak and hole (e $Å^{-3}$)	0.409 and -0.231
CCDC reference number	997585

Theoretical Studies

Lattice energy and intermolecular interaction energies partitioned into coulombic, polarization, dispersion and repulsion energy terms were evaluated using the PIXEL method present in the CLP module.[73-75] Similar calculations have been utilized in several related studies.[76-77] Electrostatic potential maps (MESP) were plotted on the Hirshfeld surface at B3LYP/6-311G** with potentials ranging from -0.06 au (red) to 0.06 au (blue) using Crystal Explorer (version 17.5).[78] This program was also used for mapping 2D fingerprint plots[79-80] to help with evaluating the contribution of the different intermolecular interactions present in a molecule in a crystalline environment. Analysis of

View Article Online
DOI: 10.1039/C7CE01310H

similarity and dissimilarity between the reported structures was performed using XPac2.0[81-82] which helps in identifying 0D, 1D, 2D or 3D supramolecular constructs (SC) for a pair of molecule. It also provides information on the extent of dissimilarity (dissimilarity index 'x') as well as the dissimilarity parameters such as the stretch parameter 'D'. For XPac analysis, we have taken all of the atomic co- ordinates (in crystal geometry) of the amide bonds and the rings carbon atoms.

CSD Search

CSD version 5.38 (Nov 2016)[83] was used to identify previously reported N-(substituted phenyl)-2-naphthamide derivatives. Only organic structures whose 3D coordinates are determined and are not disordered, ionic, polymeric, and have no errors were included in the search. Powder structures were also excluded from the search together with limiting the search to structures with R-factors < 0.1.

Result and Discussion

Molecular Structure and Conformation

ORTEP diagrams of all the seven structures are presented in Figure 1. The molecular structure of each the compounds comprises a planar napathamide ring system linked by a C(=O)NH amide unit to a phenyl or substituted phenyl ring except in the case of **2** where the second molecular component is a cyclohexane ring. All the molecules have two kinds of hydrogen bond donors [N-H, C-H]. The majority of the C-H donors are the $C(sp^2)$_H donors of the aromatic rings while molecules **3**, **4**, **5** additionally provide $C(sp^3)$-H donors. Oxygen atoms from the O=C and O-CH_3 groups or the π-electron clouds of the aromatic rings can act as hydrogen bond acceptors in the various systems. The presence of π- electron clouds can also result in the π···π stacking interactions being involved in the crystal packing. The chlorine atom present in **4** can participate, in either hydrogen or a halogen bonding. With the exception of **5** all of the compounds crystallise with one molecule in the asymmetric unit. **5** on the other hand has two molecules in the asymmetric unit that are linked by N-H···O and C-H···O interactions in addition to an offset π···π interaction [Figure 1(e)]. The molecular conformation of **7** [Figure 1(g)] was stabilized by the formation of an intramolecular N-H···O hydrogen bond [$d_{H...O}$: 2.00Å ; $\angle_{N-H...O}$: 134°].

View Article Online
DOI: 10.1039/C7CE01310H

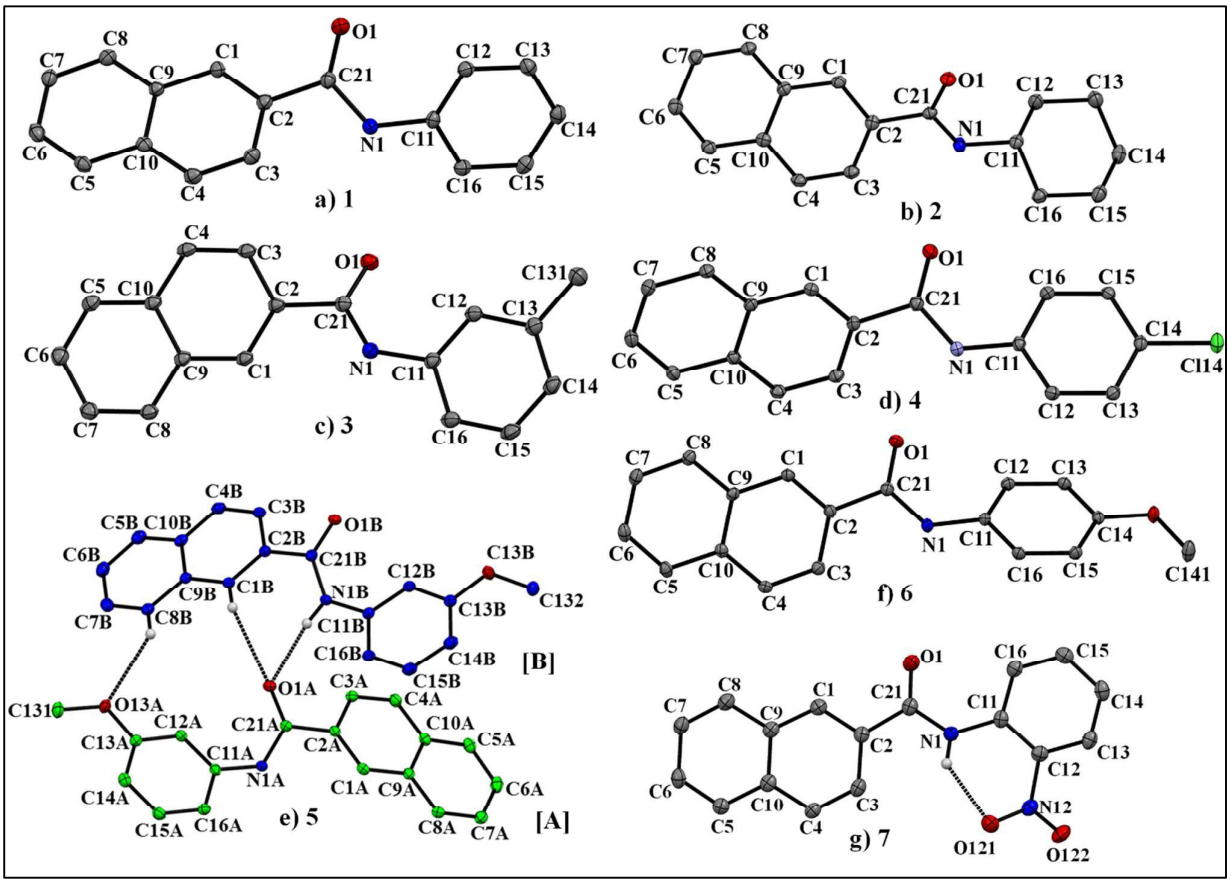

Figure 1: ORTEP plots for a) **1** b) **2** c) **3** d) **4** e) **5** f) **6** g) **7** with ellipsoids for the non-hydrogen atoms drawn with the 50% ellipsoidal probability level.

The overlay diagram [Figure 2] of all the structures reveals the considerable conformational flexibility between these structures. The magnitudes of the three major torsional angles in each of the structures are shown in Table 2. The magnitude of τ_2 representing the torsion about the amide bond was largely unaffected by the molecular environment, falling in the narrow range of 172-180°. τ_1 and τ_3 had similar magnitudes in case of **1, 2, 4** and **6** with magnitudes ranging from 149-153° (τ_1) and 148-159 (τ_3), respectively. In case of **3** and **5**, τ_2 was significantly less while τ_3 remain unaffected suggesting the rotation of the molecule via naphthalene ring to give nearly planar molecules. In the case of **7** however, the magnitudes of the τ_3 [21°] and τ_1 [168°] angles are reversed in comparison to those for **3** and **5** but with the molecule remaining reasonable planar, excluding the NO_2 substituent. Here an oxygen atom of the $-NO_2$ group avoids steric hindrance with the O=C group of the amide bond [Figure 1(g)] and instead stabilizes the molecular structure by forming a strong intramolecular N-H···O hydrogen bond.

View Article Online
DOI: 10.1039/C7CE01310H

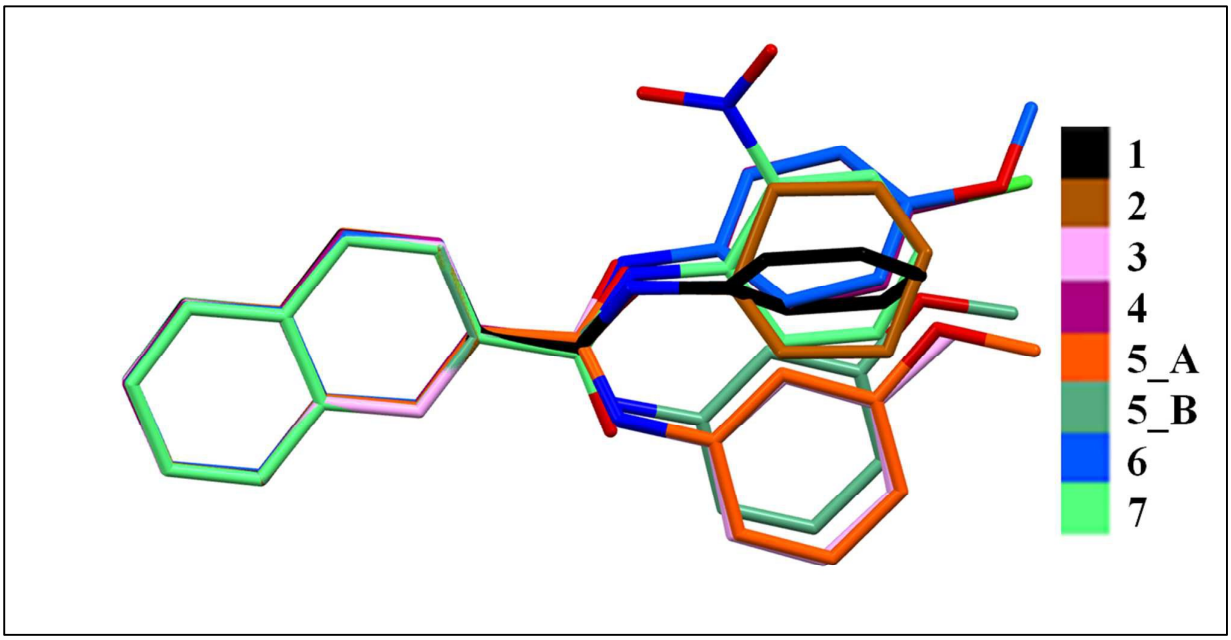

Figure 2: Molecular overlay diagram of the crystal structures of **1-7** with respective color codes.

Table 2: Magnitude of important torsions τ_1, τ_2, τ_3 in molecules 1-7.

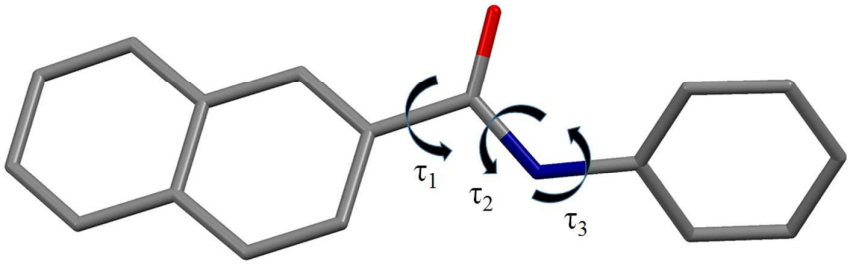

Code	τ_1(N1-C21-C2-C1)	τ_2 (C2-C21-N1-C11)	τ_3(C21-N1-C11-C16)
1	149.0(1)	178.2(1)	149.6(1)
2	155.5(1)	178.5(1)	147.7(1)
3	26.8(1)	176.1(1)	156.3(1)
4	153.7(4)	173.7(5)	158.6(5)
5_A	34.4(1)	179.5(1)	147.8(1)
5_B	32.4(1)	179.8(1)	150.9(1)
6	153.2(1)	171.9(1)	159.0(1)
7	167.9(1)	177.2(1)	20.6(1)

View Article Online
DOI: 10.1039/C7CE01310H

Lattice Energy and Electrostatic Potential Maps

Table 3: Lattice Energies of structures **1-7**(kJ/mol).

Code	E_{coul}	E_{pol}	E_{disp}	E_{rep}	E_{total}
1	-62.4	-30.7	-190.7	130.2	-153.6
2	-61.2	-28.4	-184.0	129.2	-144.4
3	-79.2	-40.7	-185.9	151.6	-154.2
4	-70.5	-27.7	-199.5	136.7	-161.0
5	-86.5	-40.7	-194.7	156.1	-165.8
6	-75.3	-38.6	-210.6	155.1	-169.6
7	-45.1	-19.6	-191.0	119.0	-136.6

Table 3 shows the calculated lattice energies for the crystal structures reported here with magnitudes ranging from -136.6 kJ/mol (**7**) to -169.6 kJ/mol (**6**). It is clearly evident that presence of a phenyl ring in (**1**) provides somewhat more stability to the lattice than a cyclohexane ring in (**2**). Also, the presence of different substituents i.e. $–CH_3$ (**3**) $–OCH_3$ (**5, 6**) and –Cl (**4**) substituents results in relatively large lattice energies. The presence of additional substituents can lead to presence of additional intermolecular interactions which inturn can lead to additional lattice stability. However in case of **7**, the presence of o-NO_2 group resulted in decrease in overall lattice energy due to significantly lower contribution from the E_{elec} and E_{pol} energy components. The presence of an intramolecular N-H···O interaction can be attributed to this decrease in case of **7**. The dispersion energy was the largest contributor towards the stability of the lattice with percentage contribution towards stabilization ranging from 60% (**5**) to 75% (**7**). [The percentage contribution towards stabilization was calculated by adding the contribution of individual stabilization components (coulombic + polarization + dispersion) with the total of stabilization terms]. The largest 40% contribution towards stabilization obtained from E_{coul} and E_{pol} in **5** can be attributed to the presence of two molecules in the asymmetric unit which can result in more electrostatic driven interactions in the lattice.

The Molecular Electrostatic Potential (MESP) maps show that the π-region of the naphthalene ring **(in red, marked as region A) [**Figure 3**]** have negative electrostatic regions for all of the molecules and hence can act as a hydrogen bond acceptors. The phenyl ring **(in red, marked as region B)** also displays a negative electrostatic region for all the molecules except **7**. In the case of **7**, the phenyl ring carries a strongly electron withdrawing -NO_2 substituent resulting in the phenyl ring being electron deficient [Figure 3(h)]. Also, as expected, the additional hydrogen atoms on the cyclohexane ring results in the region around this ring having a positive electrostatic region [Figure 3(b)].

View Article Online
DOI: 10.1039/C7CE01310H

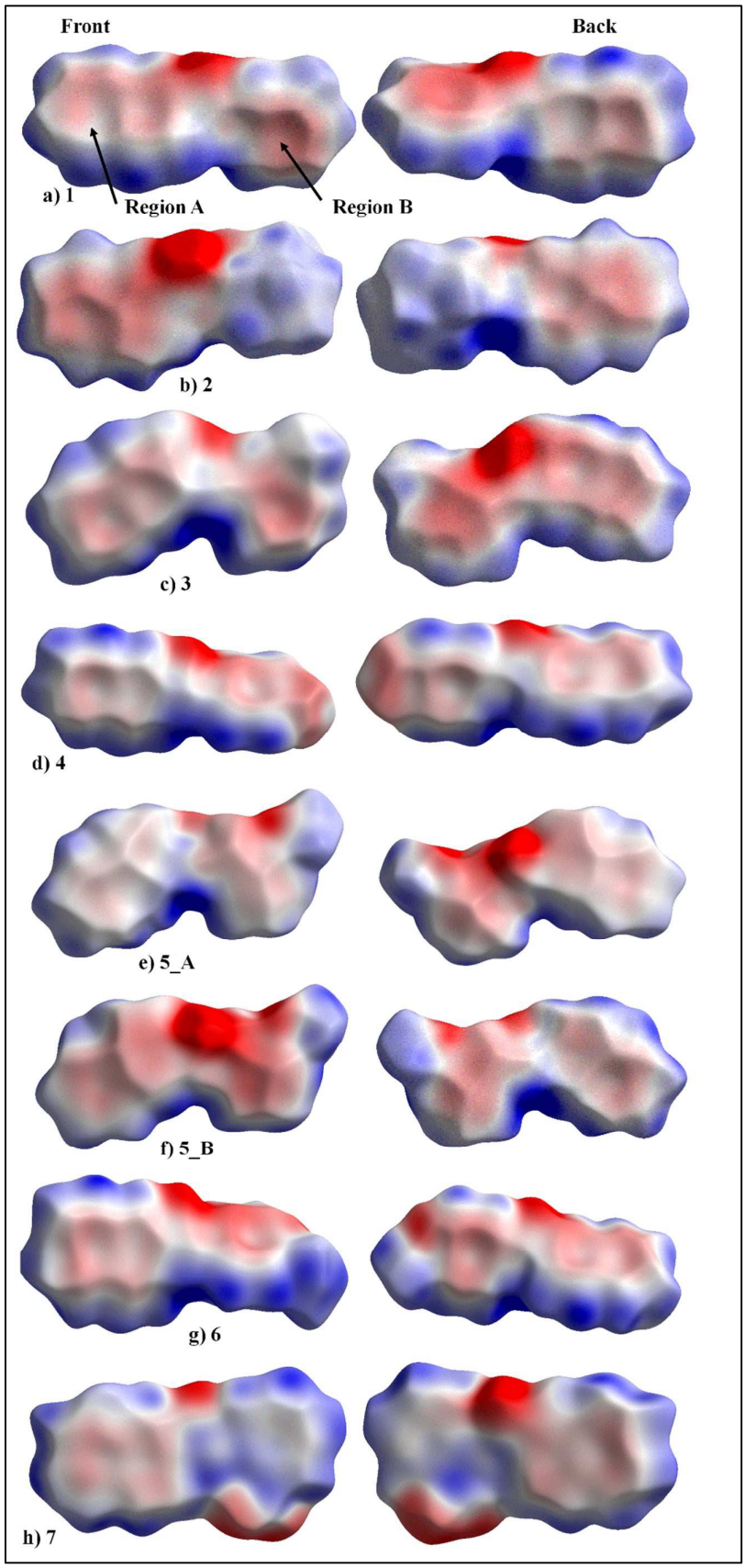

View Article Online
DOI: 10.1039/C7CE01310H

Figure 3: Molecular Electrostatic Potential Maps of a) **1** b) **2** c) **3** d) **4** e) **5_A** f) **5_B** g) **6** h) **7** drawn on Hirshfeld isosurfaces with potentials ranging from -0.06 a.u. (red) to 0.06 a.u. (blue).

Molecular Packing and Interaction Energies

Table 4 presents the intermolecular interactions present in the reported structures along with geometrical parameters and corresponding interaction energies partitioned into different energy components. Figures S1-S7 shows the important molecular pairs present in each structure and Figures 4-10 represents the molecular packing.

Table 4: List of intermolecular interactions observed in Molecule 1-7 along with interactions energies and geometrical parameters.

Motifs	Centroid-Centroid dist. (Å)	E_{coul} (kJ/mol)	E_{pol} (kJ/mol)	E_{disp} (kJ/mol)	E_{rep} (kJ/mol)	E_{total} (kJ/mol)	Symmetry Code	Intermolecular Interactions	Geometrical Parameters (Å)/(°)/(°)
Molecule 1									
I	5.480	-31.6	-9.9	-46.6	36.4	-51.7	x,-1+y,z	N1-H1N…O1 C3-H3…O1 Stacking	2.51/165 2.80/125
II	4.964	-16.1	-8.0	-53.0	37.6	-39.4	x,-y,0.5+z	C4-H4…C1(Cg1) C15-H15…C13(Cg3) C16-H16…C11(Cg3)	2.72/153 3.00/154 3.00/117
III	4.613	-12.5	-8.3	-50.1	35.9	-34.9	x,1-y,-0.5+z	C13-H13…C14(Cg3) C1-H1…C4(Cg1) C8-H8…C5(Cg2)	3.00/120 3.00/156 2.63/148
IV	13.900	-3.6	-1.1	-11.1	7.3	-8.5	-0.5+x,0.5-y,-0.5+z	C7-H7…C14(Cg3)	3.06/116
V	14.627	-0.7	-1.1	-9.9	5.3	-6.3	-0.5+x,0.5+y,z	C14-H14…H7-C7	2.62/129/114
VI	14.627	-1.8	-1.6	-10.1	7.3	-6.2	-0.5+x,-0.5+y,z	C6-H6…H14-C14	2.44/132/117
Molecule 2									
I	5.182	-37.0	-15.3	-50.6	50.4	-52.4	x-1,y,z	N1-H1N…O1 C21-O1…H16B Molecular Stacking	2.16/160 2.77/128
II	6.544	-9.6	-5.0	-46.4	29.3	-31.7	x,y-1,z	C16-H16A…C1(Cg1) C2(Cg1)…C7(Cg2)	2.90/133 3.480

View Article Online
DOI: 10.1039/C7CE01310H

								C8(Cg2)…C21	3.397(4)
III	8.347	-3.2	-3.8	-25.0	15.3	-16.7	x-1,y+1,z	C3-H3…H7-C7 C16-H16A….H1-C1	2.46/127/127 2.54/110/155
IV	10.051	-3.5	-1.5	-15.2	7.9	-12.3	-x+2,y-0.5,-z	C6-H6…C5(Cg2)	3.04/122
V	10.669	-3.0	-1.1	-14.2	9.3	-9.0	2-x,y-0.5,1-z	C12-H12A…H13B-C13 C13-H13A…H14B-C14	2.62/153/102 2.66/106/153
VI	10.383	-2.5	-2.0	-13.3	9.2	-8.6	1-x,-0.5+y,-z	C4-H4…H5-C5	2.44/129/123
VII	11.366	-2.0	-0.8	-12.4	7.8	-7.4	1-x,-0.5+y,1-z	C14-H14B…H14A-C14 C14-H14B…H12B-C12	2.66/151/130 2.68/110/129
Molecule 3									
I	4.375	-58.0	-24.4	-68.2	88.9	-61.7	x,0.5-y,-0.5+z	N1-H1N…O1 C1-H1…O1 C16-H16…O1 C131-H13B…C15(Cg3) C12-H12…C16(Cg3) C8-H8…C4(Cg1)	1.93/167 2.51/138 2.63/126 2.89/171 2.93/143 2.91/155
II	5.884	-5.9	-4.2	-39.8	20.9	-29.0	x,-1+y,z	Molecular Stacking	
III	6.716	-3.2	-3.3	-25.6	14.2	-17.8	x,1.5-y,0.5+z	C4-H4…C8(Cg2)	2.93/154
IV	7.901	-3.5	-2.2	-14.4	9.8	-10.3	x,-0.5-y,-0.5+z	C15-H15…C13(Cg3)	2.95/142
V	13.988	-2.6	-1.6	-13.1	8.4	-8.9	-x,-y,2-z	C131-H13A…H14	2.51/151
VI	13.746	-2.4	-1.4	-11.4	7.0	-8.2	1-x,0.5+y,1.5-z	C5-H5…H6-H7	2.50/152/118
Molecule 4									
I	5.599	-32.2	-9.8	-48.9	37.1	-53.7	x-1,y,z	N1-H1N…O1 C16-H16…O1 Stacking	2.53/155 2.65/133
II	4.351	-16.0	-7.3	-58.0	36.6	-44.7	1-x,-y,1-z	C12-H12…C3(Cg1) C13-H13…C5(Cg2)	2.95/153 2.91/147
III	4.613	-17.0	-8.5	-57.1	40.8	-41.8	-x,1-y,1-z	C15-H15…C8(Cg2) C16-H16…C1(Cg1)	2.90/142 2.85/144
IV	4.749	-19.4	-9.7	-60.4	48.0	-41.5	1-x,1-y,1-z	C8-H8…C15(Cg3)	2.77/154
V	5.022	-19.4	-9.1	-58.4	45.9	-40.9	-x,-y,1-z	C4-H4…C12(Cg3)	2.83/149
VI	15.867	-2.5	-0.8	-8.2	3.8	-7.7	x,y,z-1	C6-H6…Cl14	3.16/130

View Article Online
DOI: 10.1039/C7CE01310H

VII	16.276	-2.8	-1.1	-9.0	5.8	-7.1	1+x,y,z-1	C7-H7…Cl14	3.03/119
VIII	15.893	-0.8	-1.0	-7.1	7.2	-1.6	-x,-y,2-z	C14-Cl14…Cl14	3.554(1)/129
Molecule 5									
I	4.887	-48.0	-19.8	-50.0	62.8	-55.0	x,y,z	N1B-H1NB…O1A C1B-H1B…O1A C16B-H16B…O1A C8B-H8B…O13A C3A(Cg1)…C16B(Cg6)	2.09/170/ 2.48/129 2.84/128 2.49/135 3.552(2)
II	4.891	-48.7	-20.3	-51.0	65.0	-54.9	-1+x,y,z	N1A-H1NA…O1B C1A-H1A…O1B C16A-H16A…O1B C8A-H8A…O13B C16A(Cg3)…C2B(Cg4)	2.10/167/ 2.53/129 2.78/128 2.48/137 3.531(1)
III	8.184	-6.1	-5.6	-32.8	22.8	-21.6	0.5+x,1.5-y,-z	C1B-H1B…C15A(Cg3) C131-H13C…C11B(Cg6)	3.00/145 2.87/130
IV	9.553	-8.9	-3.1	-16.4	6.9	-21.5	2-x-0.5+y,0.5-z	C5A-H5A…O1B C4A-H4A…C12B(Cg6)	2.98/165 3.04/166
V	8.270	-5.2	-5.2	-32.9	23.3	-20.1	1-x,-0.5+y,0.5-z	C6A-H6A…C11A(Cg3)	2.88/137
VI	8.411	-6.7	-3.9	-26.5	18.5	-18.5	2-x,-0.5+y,0.5-z	C132-H13D…C2B(Cg4) C14B-H14B…C3B(Cg4)	2.94/141 2.83/171
VII	8.614	-6.0	-3.0	-25.1	16.5	-17.5	0.5+x,0.5-y,-z	C6B-H6B…C2A(Cg1) C5B-H5B…O1A	2.97/131 2.90/153
VIII	12.279	-11.7	-3.5	-20.0	18.2	-17.0	1.5-x,1-y,-0.5+z	C132-H13F…O13A C131-H13A…O13B	2.68/122 2.80/117
IX	9.862	-5.1	-2.4	-18.5	11.4	-14.7	0.5+x,0.5-y,-z	C3B-H3B…C6B(Cg5)	2.87/141
X	9.612	-3.4	-3.1	-16.0	7.9	-14.6	-0.5+x,1.5-y,-z	C15A-H15A…C12A(Cg3)	2.84/162
XI	9.744	-3.5	-2.2	-17.7	9.8	-13.5	1-x,0.5+y,0.5-z	C15-H15B…C9A	2.89/158
XII	12.085	-4.3	-2.3	-23.4	18.6	-11.4	1.5-x,1-y,0.5+z	C6A(Cg2)…C7B(Cg5) C7A(Cg2)…C6B(Cg5)	3.524(1) 3.543(1)
XIII	13.196	-3.6	-1.5	-13.5	8.2	-10.4	0.5-x,1-y,0.5+z	C7A-H7A…C14A(Cg3)	2.91/129
XIV	13.196	-2.8	-1.1	-11.8	5.9	-9.8	1.5-x,1-y,-0.5+z	C7B-H7B…C14B(Cg6)	2.95/136
XV	13.054	-2.9	-2.1	-11.7	8.8	-7.8	1.5-x,1-y,-0.5+z	C131-H13B…C4A(Cg1)	2.93/137

View Article Online
DOI: 10.1039/C7CE01310H

XVI	13.057	-2.0	-1.9	-10.5	7.4	-7.0	2.5-x,1-y,0.5+z	C132-H13E…C4B(Cg1)	3.02/148
Molecule 6									
I	5.516	-34.3	-11.1	-52.3	41.8	-56.0	-1+x,y,z	N1-H1N…O1 C16-H16…O1 Molecular Stacking	2.48/155 2.65/131
II	4.902	-26.4	-12.8	-65.5	59.1	-45.6	1-x,-y,-z	C5-H5…O14 C4-H4…C12(Cg3)	2.90/146 2.72/152
III	4.564	-18.9	-10.1	-63.8	47.3	-45.4	1-x,1-y,-z	C141-H14A…C6(Cg2) C15-H15…C8(Cg2) C16-H16…C1(Cg1)	2.92/162 2.93/141 2.84/147
IV	4.712	-18.0	-12.4	-61.2	51.5	-40.0	2-x,1-y,-z	C1-H1…C11(Cg3) C8-H8…C15(Cg3)	3.07/134 2.71/155
V	4.456	-12.2	-7.3	-55.3	36.0	-38.9	2-x,-y,-z	C12-H12…C4(Cg1) C13-H13…C5(Cg2)	2.99/139 2.84/150
VI	16.255	-8.0	-1.8	-9.3	6.9	-12.1	1-x,-y,1-z	C141-H14B…O14	2.70/133
VII	16.101	-1.5	-1.5	-8.4	5.1	-6.3	x,y,-1+z	C5-H5…H14B-C14 C6-H6…O14	2.47/135/150 3.02/150
Molecule 7									
I	3.388	-19.7	-8.9	-95.7	71.3	-52.9	-x,1-y,1-z	Stacking	
II	4.045	-16.7	-6.4	-86.1	57.2	-51.9	1-x,1-y,1-z	Stacking	
III	8.187	-12.7	-5.7	-24.9	17.1	-26.2	x,-1+y,z	C5-H5…O1 C4-H4…O1 C15-H12…O121	2.65/141 2.66/142 2.71/132
IV	7.532	-6.6	-3.6	-27.9	14.2	-23.9	-x,2-y,1-z	C5-H5…O121 C4(Cg1)…C4(Cg1)	2.84/125 3.687(1)
V	7.422	-5.5	-4.4	-27.2	15.0	-22.2	1-x,-y,1-z	C16-H16…O1# C1-H1…H15-C15	2.82/127 2.42/127/129
VI	11.511	-9.2	-2.0	-11.8	9.3	-13.6	-x,1-y,2-z	C13-H13…O122 N12-O122…O122	2.75/130 2.984/100
VII	14.218	-1.9	-0.7	-9.5	4.5	-7.7	x,-1+y,1+z	C6(Cg2)…C13(Cg3) C7(Cg2)…C14(Cg3)	3.896(1) 3.689(2)

Notes: Centroid-Centroid distance corresponds to the distance between the molecular centre of the interacting molecules.

Cg1 :C1-C2-C3-C4-C10-C9/C1A-C2A-C3A-C4A-C10A-C9A ; Cg2: C5-C6-C7-C8-C9-C10/C5A-C6A-C7A-C8A-C9A-

View Article Online
DOI: 10.1039/C7CE01310H

C10A ; Cg3: C11-C12-C13-C14-C15-C16/C11A-C12A-C13A-C14A-C15A-C16A ; Cg4: C1B-C2B-C3B-C4B-C10B-C9B ; Cg5: C5B-C6B-C7B-C8B-C9B-C10B ; Cg6: C11B-C12B-C13B-C14B-C15B-C16B.

Packing of 1

The molecule **1** crystallizes in triclinic space group *P*-1 with Z =2 [Figure 4]. The most stabilized molecular contact resulted from a strong and directional N-H···O=C [$d_{N...O}$: 2.51 Å; $\angle_{N-H...O}$: 165°] interaction leading to the formation of a molecular chain along the *b*-axis [motif **I**, Figure 4(a)]. Motif **I** was additionally supported by C-H···O [2.80 Å; 125°] and molecular stacking [involving atoms of the Cg1, Cg2 and Cg3 rings] resulting in a total interaction energy of -51.7 kJ/mol [Table 4]. The strong N-H···O hydrogen bond makes a significant contribution of electrostatic energy [coulombic + polarization] towards stabilization [~41%]. The dispersion contribution [~59%] was also significant due to the presence of π···π stacking. As observed in the MESP analysis [Figure 3(a)], the aromatic rings present in the structure of **1** have regions of highly negative electrostatic potential and, as expected, this resulted in presence of multiple motifs stabilized by multiple C-H···π interactions [Figure 4(a)]. Perpendicular to the *bc*-plain, chains formed by motif **I** are interlinked by motifs **II** and **III** consisting of T-shaped C-H···π interactions (involving atoms of Cg1, Cg2 and Cg3 rings)) [Figure 4(a)]. The H···C(π) distances were always less than 3 Å in these two motifs [Table 4]. The interaction energies for motifs **II** and **III** were calculated to be -39.4 kJ/mol and -34.9 kJ/mol, respectively with large contributions to stabilisation from the dispersion energy components [Table 4]. In previous theoretical studies,[84] it has been shown that the interaction energy of a single C-H···π interaction can be as high as -10 kJ/mol in the optimized state. In crystals, the molecular environment around the C-H···π contact becomes important and can contribute towards the dispersion energy resulting in higher stabilisation. Along the *a*-axis also, chains formed through motif **I** were further interconnected by motif **IV** (-8.5 kJ/mol, a C-H···π interaction), **V** (-6.3 kJ/mol, an H···H interaction) and **VI** (-6.2 kJ/mol, an H···H interaction) [Figure 4(b)]. These motifs were highly dispersive in nature with contributions of more than 70% towards stabilization. The weak and highly dispersive nature of these three motifs suggests that they are largely a consequence of crystal packing.

View Article Online
DOI: 10.1039/C7CE01310H

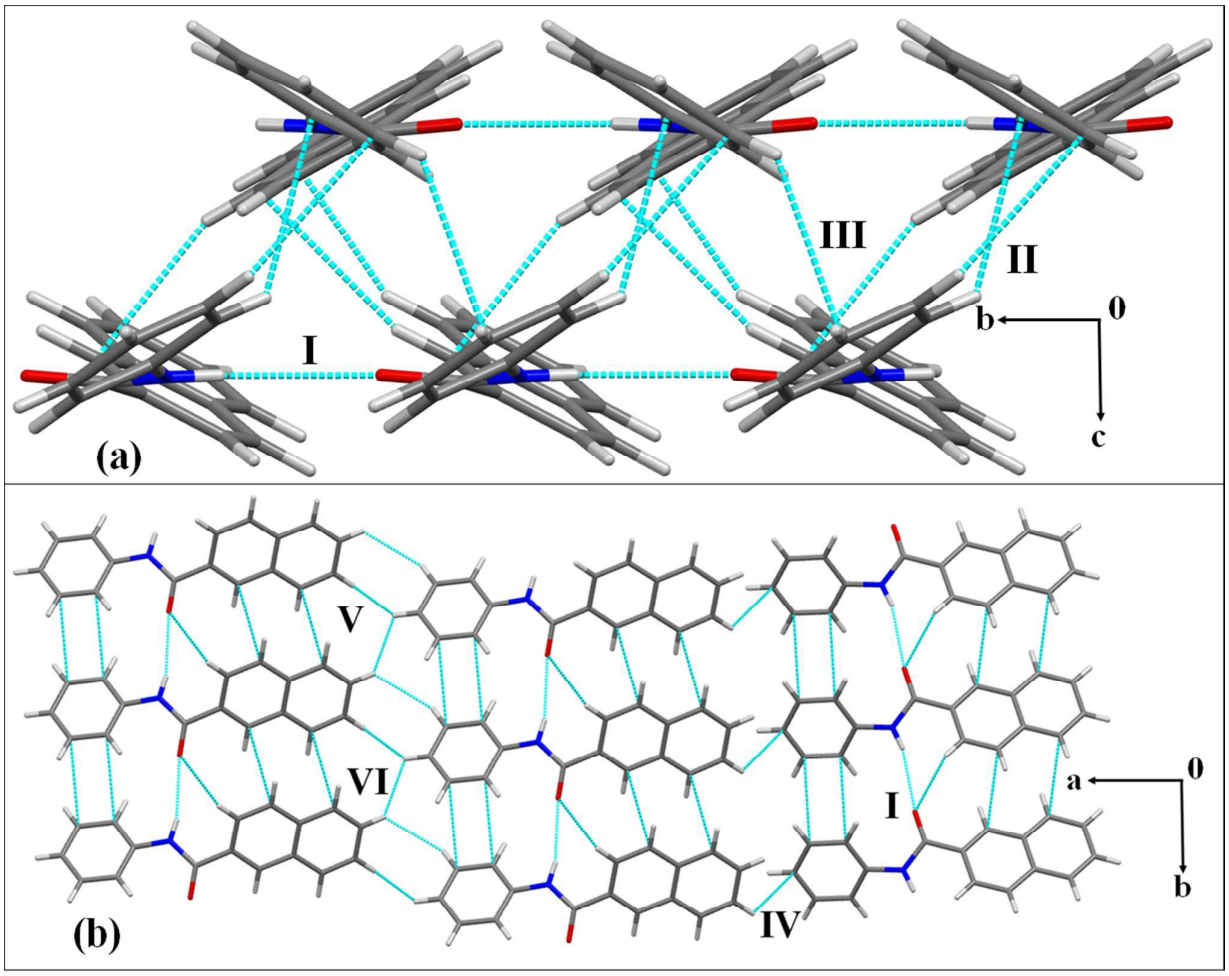

Figure 4: Packing diagram of 1 showing the nature of (a) motifs **I, II, III** and (b) **IV, V** and **VI.**

Packing of 2

Molecule **2** crystallizes in the monoclinic space group $P2_1$ with Z=2. The presence of a cyclohexane ring, in place of the phenyl ring in **1** [Figure 1(b)], results in the presence of additional positive electrostatic regions [**Region B**, Figure 3(b)]. The molecular packing in **2** is therefore significantly different to that found in **1** [Figure 5(a)-(b)]. Motif **I** forms a molecular chain along the *a*-axis through a short and directional N-H···O=C hydrogen bond [$d_{N...O}$: 2.16 Å; $\angle_{N-H...O}$: 160°] with additional stability provided by C-H···O [$d_{H...O}$: 2.77 Å; $\angle_{C-H...O}$: 128°] interaction and molecular stacking [involving Cg1, Cg2 and Cg3]. The interaction energy of motif **I** was calculated to -52.4 kJ/mol [Table 4] with comparable contributions from the electrostatic [51%] and dispersion energy [49%] components towards the stabilization [Table 4]. Motif **II** consisted of a C-H···π(Cg1) interaction which is augmented by π···π interactions [involving Cg1, Cg2 and Cg3]. This motif was again highly dispersive with an approximately 76% contribution towards stabilization. Another

View Article Online
DOI: 10.1039/C7CE01310H

highly dispersive C-H···π(Cg2) contact [motif **IV**, -12.3 kJ/mol] stabilizes the packing along the *b*-axis. The cyclohexane ring was expected to be actively involved in the formation of highly dispersive H···H contacts [Figure 5(a) and (b)]. Motif **III** [-16.7 kJ/mol], **V**[-19.0 kJ/mol], **VI** [-8.6 kJ/mol], and **VII** [-7.4 kJ/mol], all involved H···H interactions although not exclusively emanating from the cyclohexane ring. The overall contribution of dispersion towards stabilization was in excess of ~75% from these motifs . The H···H distance in these contacts ranged from 2.44 – 2.68 Å.

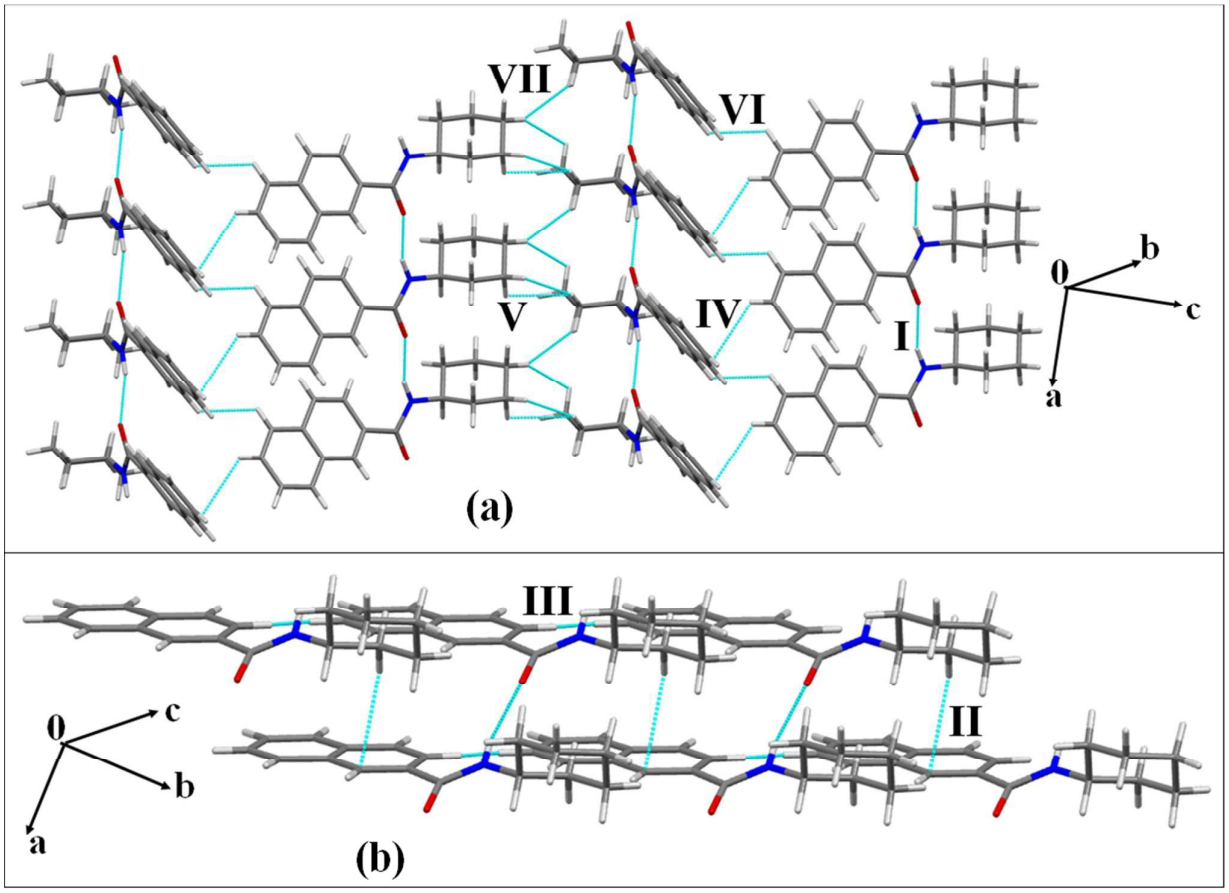

Figure 5: Packing diagram of **2** showing the nature of (a) motifs **I, IV, V, VI** and **VII** (b) **II** and **III.**

Packing of 3

Molecule **3** crystallizes in monoclinic space group $P2_1/c$ with Z=4. Unlike other molecules, motif I resulting from the N-H···O=C hydrogen bond [$d_{H...O}$: 1.93 Å; $\angle_{N-H...O}$: 167°] forms a zig-zag arrangement with molecules linked along *c* rather than a molecular chain [Fig. 6(a)]. This was also the shortest N-H···O interaction observed among the molecules reported in this study [Table 4]. As with the other molecules, motif **I** was additionally supported by a number of C-H···O and C-H···π interactions with an interaction energy of -61.7 kJ/mol. This was distributed between electrostatic,

View Article Online
DOI: 10.1039/C7CE01310H

~55% and dispersive ~45% contributions to the stabilization. Motif **II** [-29.0 kJ/mol] consisted of offset π···π interactions [involving atoms of the Cg1, Cg2 and Cg3 rings] which were highly dispersive in nature with ~80% contribution towards stabilization. Motif **III** [-17.8 kJ/mol] and **IV** [-10.3 kJ/mol], and which were due exclusively to C-H···π hydrogen bonds (involving the Cg2 and Cg3 rings) [Figure 6(b)-(c)] further stabilised the packing. The H···C (π) distances in these interactions were in the range 2.93-2.95 Å with C-H···C(π) angles in the range being 142° and 154° [Table 4]. Further stability perpendicular to the *ac*-plane [Figure 6(c)] was provided by the presence of two different but highly dispersive [>75%] H···H interactions [motif **V**, -8.9 kJ/mol; motif **VI**, -8.2 kJ/mol].

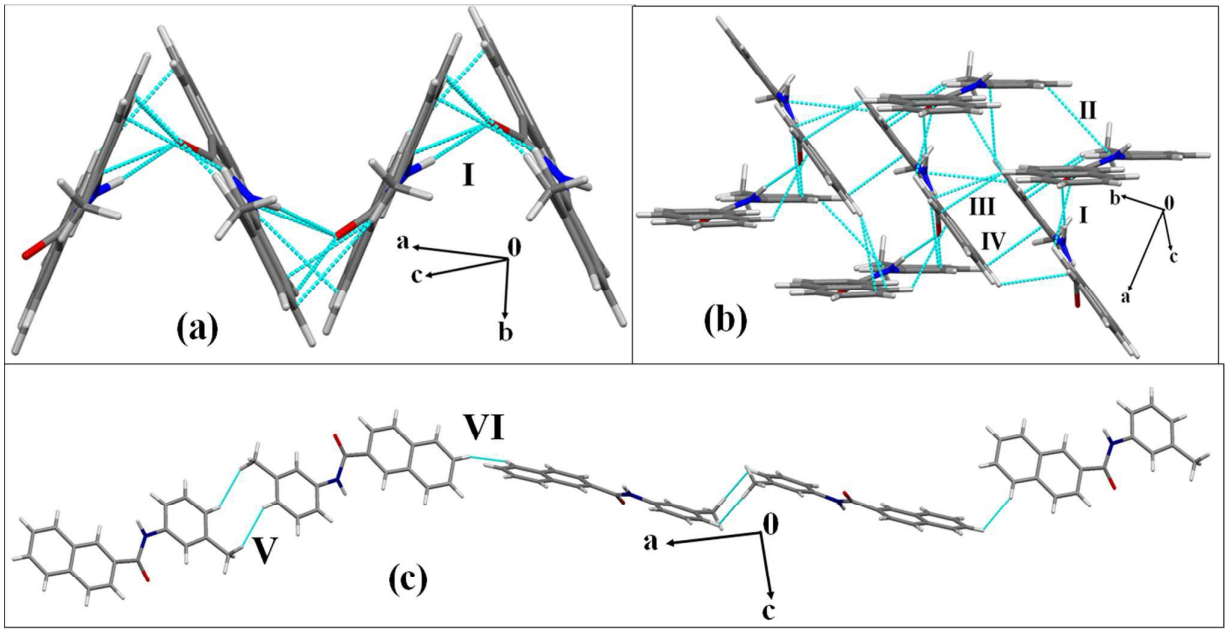

Figure 6: Packing diagram of **3** showing the nature of (a) motifs **I** (b) **II, III** and **IV** (c) **V** and **VI.**

Packing of 4

Molecule **4** crystallizes in triclinic space group *P*-1 with Z=2. The molecular packing [Figure 7(a)-(b)] was very similar to that for **1** with molecular chains formed by N-H···O=C hydrogen bonds and interconnected further [Figure 7(b)] by various motifs including several C-H···π contacts (involving atoms of the Cg1, Cg2 and Cg3 rings) [motifs **II – V**, Figure 7(b)]. The energy of each of these motifs was > 40 kJ/mol with dispersion being the dominant contributor towards stabilization [Table 4]. However, the unique feature of the molecular packing of **4** was the participation of the Cl atom in forming both hydrogen [Figure 7(c)] and halogen bonds [Figure 7(b)]. Motifs VI [-7.7 kJ/mol] and VII [-7.1 kJ/mol] result from two discrete C6-H6···Cl14 and C7-H7···Cl14 hydrogen bonds that

View Article Online
DOI: 10.1039/C7CE01310H

combine with the N-H···O contact, motif **1**,to generate sheets of molecules in the *ac* plane, Fig 7(c). The Cl···Cl halogen bonds, motif **VIII**, form dimers that are linked into double chains along *a* by the N-H···O hydrogen bonds, Fig 7(a). These C-H···Cl hydrogen bonds were highly dispersive in nature with contributions towards stabilization of ~70% in both motifs, **VI** and **VII**. The Cl···Cl halogen bond was also a dispersive Type I interaction[85] [$d_{Cl...Cl}$: 3.554(1) Å; $\angle_{C\text{-}Cl...Cl}$: 129°]. However this contact is weak; despite the Cl···Cl distance being less than the sum of vdW radii of the two Cl atoms.[86] the interaction energy was observed to be only -1.9 kJ/mol.

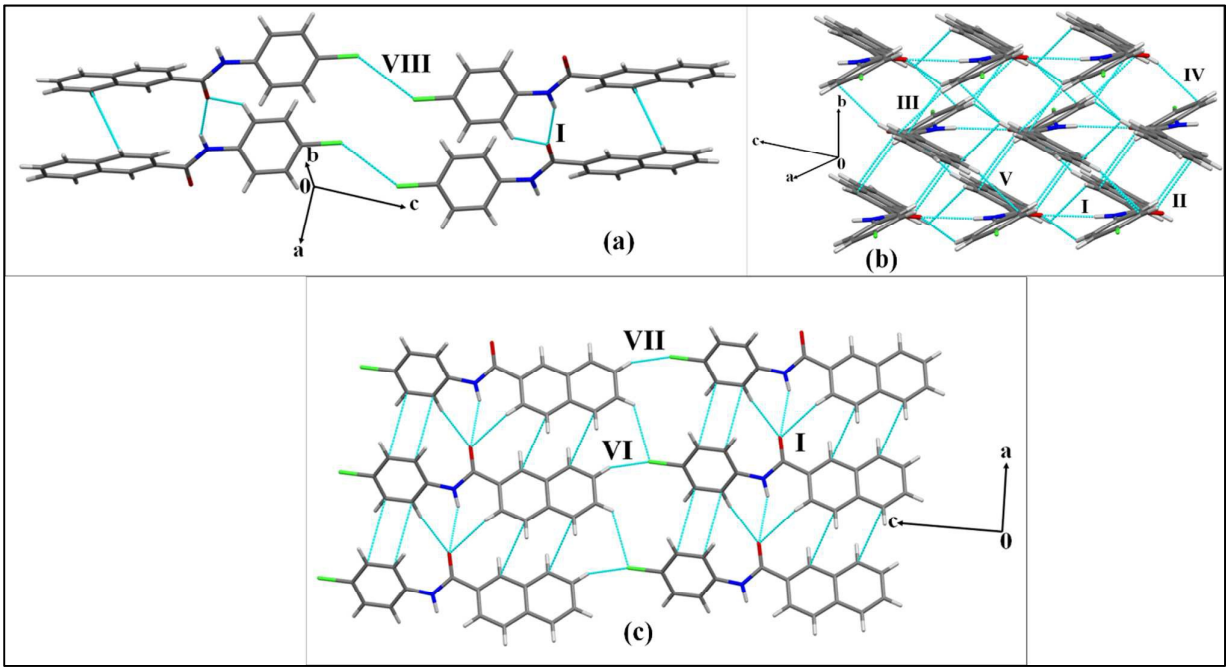

Figure 7: Packing diagram of **4** showing the nature of (a) motifs **VIII** (b) **I**, **II, III**, **IV** and **V** (c) **VI** and **VII.**

Packing of 5

The two unique molecules of 5 crystallize in the orthorhombic space group $P2_12_12_1$ with Z=8. The presence of two molecules in the asymmetric unit resulted in extremely complicated molecular packing interactions [Figure 8(a)-(c)]. In the *ac*-plane, the packing is stabilized by formation of chains generated by motif **I** [-55.0 kJ/mol] and motif **II** [-54.9 kJ/mol] contacts. These resulted from alternating N-H···O interactions between the two unique molecules in the asymmetric unit. These contacts were stabilised further by various C-H···O and π···π stacking interactions [Table 4]. In three dimensions packing was extensively supported by the presence of eleven different motifs each

View Article Online
DOI: 10.1039/C7CE01310H

exclusively consisting of C-H···π contacts (involving atoms of the Cg1-Cg6 rings in different motifs). The interaction energies in these eleven motifs range from -21.6 kJ/mol to -7.0 kJ/mol with dispersion contributing more than 60% towards the stabilization of the molecular pairs [Table 4]. Motifs IV [-21.5 kJ/mol] and VII [-17.5 kJ/mol] also included C-H···π hydrogen bonds (Cg1 and Cg6 rings) but these were additionally supported by C-H···O hydrogen bonds involving the oxygen atom of the carbonyl group. The oxygen atoms of the methoxy groups in both molecules are involved in similar C131-H13A···O13B and C132-H13F···O13A hydrogen bonds [motif VIII, -17.0 kJ/mol]. Stabilisation of this motif has substantial contribution from the electrostatic component. Motif XII [-11.4 kJ/mol] consisted of a π···π stacking interaction involving the atoms of the Cg1 ring with C···C distance being ~3.5Å.

View Article Online
DOI: 10.1039/C7CE01310H

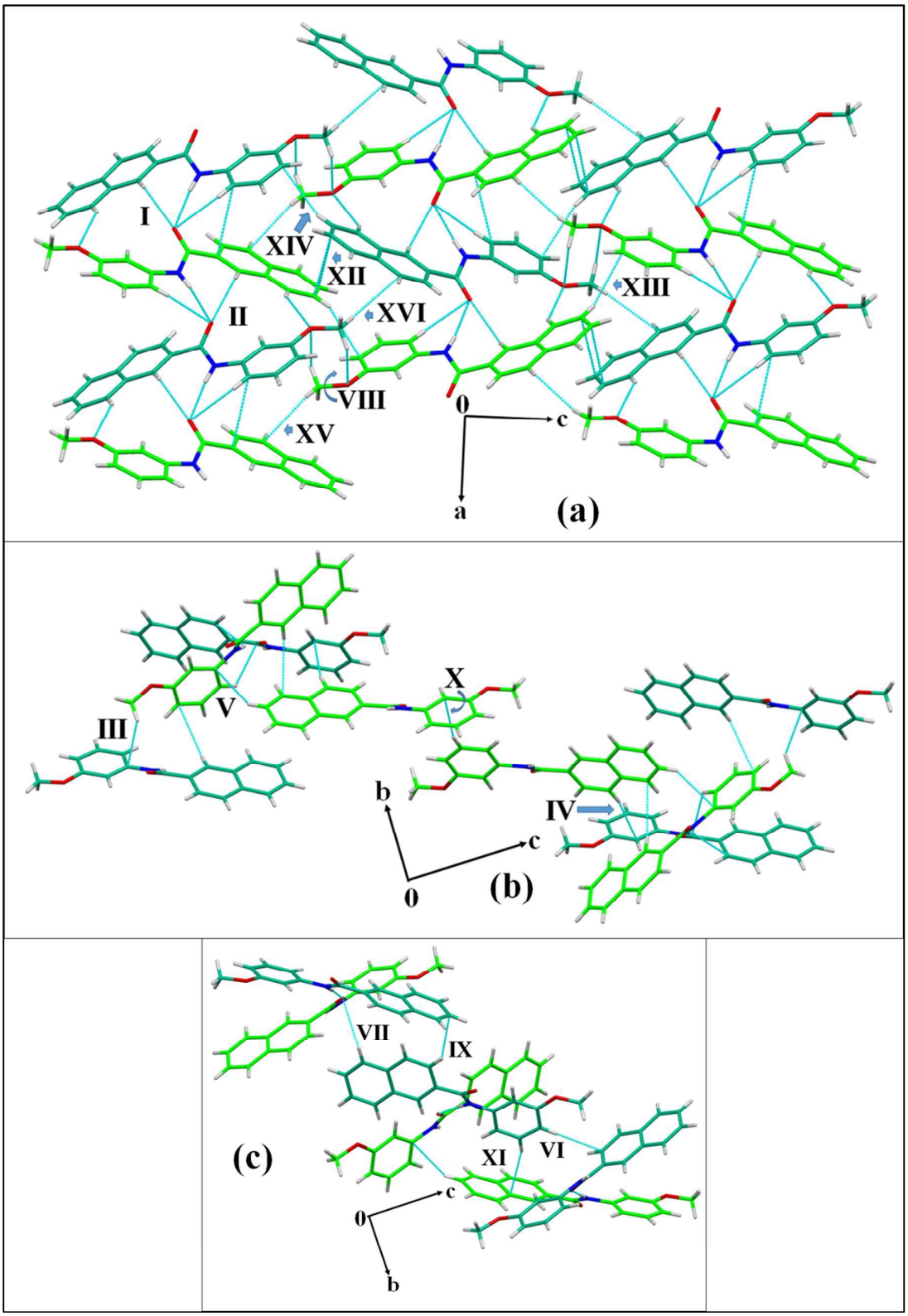

Figure 8: Packing diagram of **5** showing the nature of (a) motifs **I, II, VIII, XI, XIII, XIV, XV** and **XVI** (b) **III, IV, V** and **X** (c) **VI, VII, IX** and **XII.**

View Article Online
DOI: 10.1039/C7CE01310H

Packing of 6

Molecule **6** crystallizes in the triclinic space group *P*-1 with Z =2. The packing of **6** is largely similar to those observed for **1** and **4** again involving chains formed by the N-H···O=C hydrogen bonds [motif **I**, -56.0 kJ/mol] interconnected by several highly stabilized and dispersive motifs [**II** (-45.6 kJ/mol), **III** (-45.4 kJ/mol), **IV**(-40.0 kJ/mol) and **V**(-38.9 kJ/mol) consisting of different C-H···π interactions [Figure 9(a)-(b)]. In motif **II** the C-H···π contact (Cg3 ring) is augmented by a C-H···O hydrogen bond [$d_{H...O}$: 2.90 Å; $\angle_{C-H...O}$: 146°]. In the *bc*-plane, additional C-H···O hydrogen bonds, motif **VI** [-12.1 kJ/mol] and **VII** [-6.3 kJ/mol] gave additional stability to the molecular packing [Figure 9(b). Motif **VI** has a significant stabilising contribution from both electrostatic and dispersive energy components [Table 4], while motif **VII** was highly dispersive (> 75%) due to the relatively large intermolecular H···O distance [3.02 Å, Table 4].

View Article Online
DOI: 10.1039/C7CE01310H

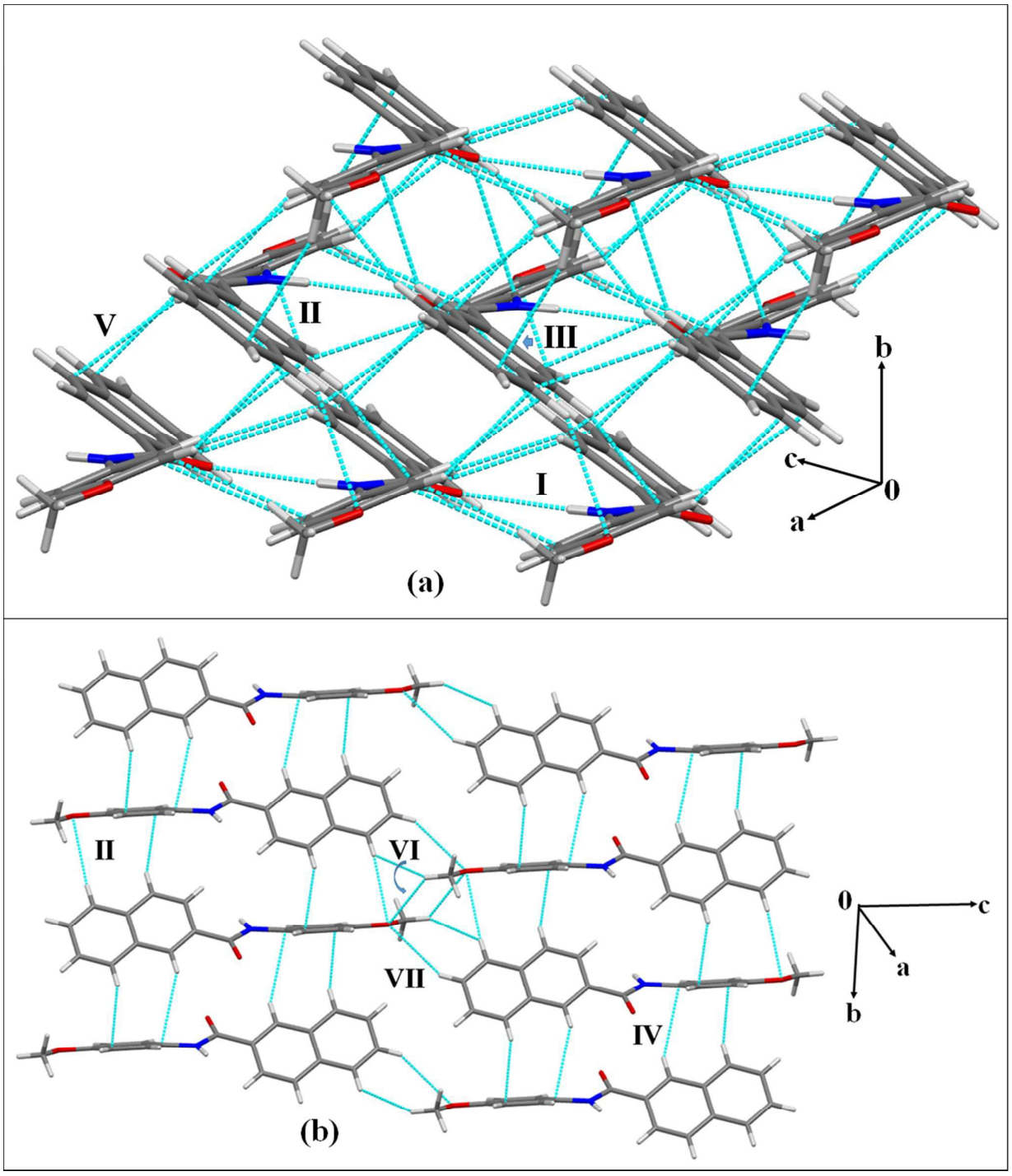

Figure 9: Packing diagram of 6 showing the nature of (a) motifs **I, II, III and V** and (b) **IV**, **VI** and **VII.**

Packing of 7

Molecule **7** crystallizes in the triclinic space group *P*-1 with Z=2. The unique feature of the crystal structure of this molecule is the absence of the strong N-H···O=C interaction seen in the other

View Article Online
DOI: 10.1039/C7CE01310H

compounds reported here. This is because of the *o*-substituted phenyl ring where the formation of intramolecular N-H···O interaction [Figure 1(g)] involving the $–NO_2$ substituent precludes the formation of the intermolecular N-H···O hydrogen bond. Also, it was observed in the MESP map of this molecule, that the phenyl ring was clearly electron deficient [Figure 3(h), **region B**] resulting in a high propensity for π···π stacking interactions rather than the C-H···π interactions that were prevalent in the related molecules **1**-**6** [Table 4]. Along the a-axis, the packing is stabilized by two extensive molecular stacking interactions **[Figure 10(a)].** The interaction energies of these two motifs were -52.9 kJ/mol (motif **I**) and -51.9 kJ/mol (motif **II**), respectively with dispersion being the highly dominant contribution towards stabilization being more than 75% of the total in both cases. Another weak and dispersive π(C6) ···π(C13) interaction occurs along the a-axis with an interaction energy of only -7.7 kJ/mol [motif III, Figure 10(a)]. The presence of three oxygen atoms in the molecule results in the formation of multiple C-H···O interactions which further stabilized the packing in both the *ac* and *bc* planes [Table 4]. Motif **III** [-26.2 kJ/mol] consisted of three different C-H···O interactions where the H···O distance were less than the sum of vdW radii of H and O and the interaction energies have significant contributions from both the electrostatic and dispersion energy components towards stabilization [Table 4]. Motifs **IV** [-23.9 kJ/mol] and **V** [-22.2 kJ/mol] also result from C-H···O interactions with further stability provided by the presence of additional π···π and H···H interactions, respectively [Table 4]. These motifs make significant contributions to the dispersion energy of the system. The $–NO_2$ group is also involved in the formation of an inversion dimer through C13-H13···O122 hydrogen bonds. These contacts enclose an $R^2_2(10)$ ring and have an interaction energy of -13.6 kJ/mol. Another unique feature of this motif is that the centrosymmetric interaction necessitates an additional close O···O contact [$d_{O...O}$: 2.984(3) Å; $\angle_{N-O...O}$: 100°] as a result of which, this motif has a significant contribution from dispersion [~51%] towards its stabilization [Figure 10(b)].

View Article Online
DOI: 10.1039/C7CE01310H

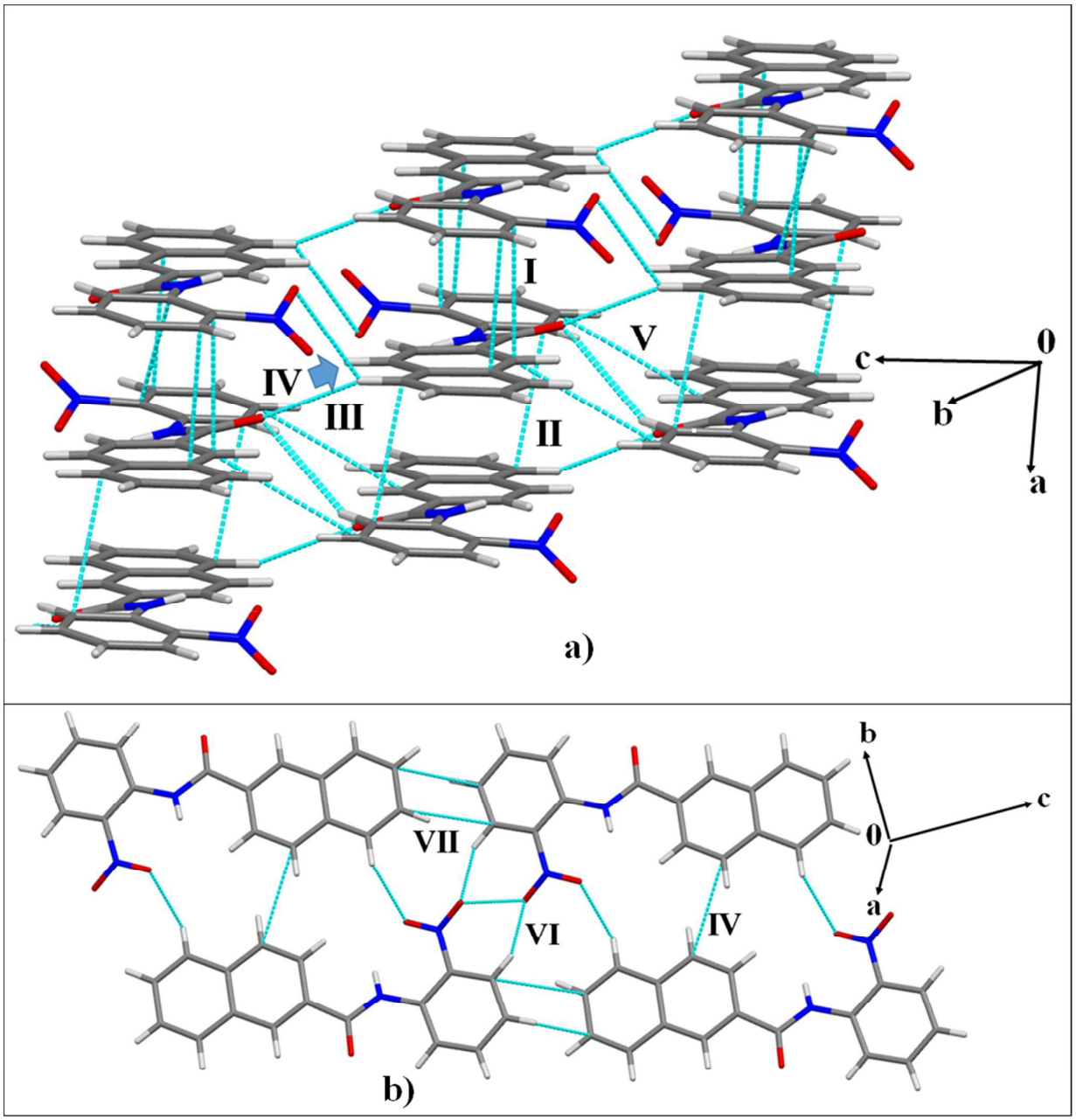

Figure 10: Packing diagram of 7 showing the nature of (a) motifs **I, II, III, IV and V** and (b) **VI** and **VII.**

Analysis of Isostructural features

It was clearly evident from the analysis of crystal packing that there are significant similarities between the molecular arrangements in molecules **1 [Figure 4]**, **4** [**Figure 7**] and **6 [Figure 9]**. Therefore, it was interesting to quantitatively investigate whether any 1D-, 2D- or 3-D similarities existed between these structures. A comparison of **1** and **4** revealed the presence of a 1D

View Article Online
DOI: 10.1039/C7CE01310H

supramolecular construct (SC) with x = 7.8 and D = 0.12 Å [Figure S8]. This 1D similarity is principally due to the formation of molecular chains through the N-H···O interactions found in both molecules. A similar 1-dimensional-supramolecular construct, 1D-SC, is also found between **1** and **6** with x and D being 8.4 and 0.04 Å [Figure S9]. Comparison of **4** and **6** reveals the presence of a 3D-SC with x = 0.21 and D =5.5 Å [Figure S10]. This similarity was largely due to the fact that **4** and **6** both crystallize in the same space group with reasonably similar cell parameters [Table 1]. No degree of supramolecular construct was observed for any other pairs of molecules in the series.

2Dimensional Fingerprint Plots

The results from the 2D Fingerprint plots [Figure 11] for **1-7** reveal that the contributions of H···C interactions to the structural stability ranged from 10.8% (in 7) to 46% (in 1) while that from H···H contacts ranged from 26.6% (in 4) to 63.7% (in 2). The H···C contacts were the major contributors to the packing in the case of **1**, **4** and **6** owing to the presence of extensive networks of C-H···π interactions. Molecule 2 had an H···C contribution of 24.3% but this was overshadowed by the H···H contribution (63.7%) due to the presence of a cyclohexane ring in place of the phenyl rings found in the other molecules. The contribution of H···H (46.2%) was slightly higher than H···C (42.4%) in **3** due to the–CH_3 substituent on the phenyl ring. Molecule **5** with two molecules in the asymmetric unit had an abundance of H···H interactions (45%) compared to H···C contacts (38.7%). As discussed earlier, the absence of a strong N-H···O hydrogen bond resulted in the packing of **7** being stabilized by π···π stacking interactions rather than C-H···π hydrogen bonds. This resulted in the contribution of C···C (16.8%) being higher than H···C (10.8%) interactions. It is also interesting to note that the contribution of C···C was observed to be significant only in the case of **7**. Also, the high contribution of H···H (38.0%) contacts in **7** in comparison to H···C interactions can be attributed to the absence of C-H···π interactions rather than a much higher propensity for H···H contacts. Indeed when compared to other molecules, the contribution of H···H in **7** was second lowest behind those observed in molecule **4**. The low magnitude of H···H (26.4%) in **4** was due to the presence of a Cl substituent in the molecule resulting in significant C-H···Cl hydrogen bond formation with a contribution of 15.1% from these H···Cl interactions [Table S1]. The contribution of O···H hydrogen bonds ranged from 8.0% (in 1) to 27.1% (in 7). Inevitably, the strong N-H···O hydrogen bonds were the major source of these O···H contributions in molecule 1-6. For **7**, the large 27.1% contribution results from the presence of the -NO_2 substituent whose oxygen atoms actively participate in forming multiple C-H···O hydrogen bonds. The combined contribution of all the

View Article Online
DOI: 10.1039/C7CE01310H

remaining interactions towards the 2-D fingerprint plots was less than 5% in each of the reported crystal structures.

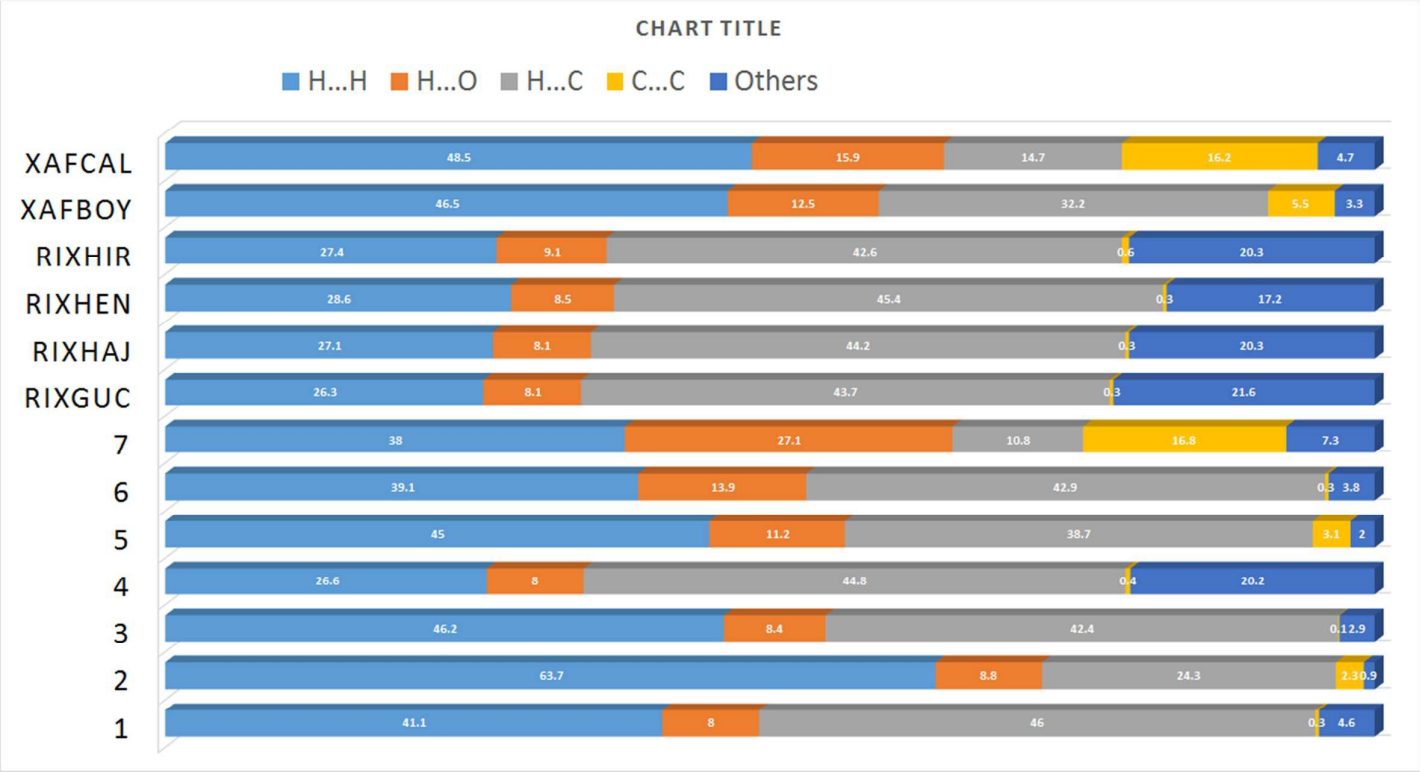

Figure 11: Percentage contributions of different intermolecular interactions in 1-7 and for several related structures retrieved from the CSD Database.

CSD Search for N-(substituted phenyl)-2-naphthamide derivatives

A search of the CSD (give version number and number of updates) for derivatives of N-(substituted phenyl)-2-naphthamide derivatives reveals the presence of only six unique additional structures with REFCODES: RIXGUC, RIXHAJ, RIXHEN, RIXHIR, XAFBOY and XAFCAL [Figure S11].[87-88] The first four structures all had of halo-substituents at the *para*-position of the phenyl ring. Similar to the structures reported here, these four compounds also formed molecular chains through strong N-H···O hydrogen bonds. XAFBOY and XAFCAL had o–CH_2OH and o–CHO substituents on the benzene ring, creating steric hindrance that prevents the formation of N-H···O hydrogen bonds, a situation comparable to that found for molecule **7**. Analysing the 2D Fingerprint plots for these six additional structures show many similar characteristics to those reported here [Figure S12]. While the halogen substituted structures [RIXGUC, RIXHAJ, RIXHEN, RIXHIR] shows significant H···C contributions, the presence of the o-substituted phenyl rings in XAFBOY and XAFCAL resulted in

View Article Online
DOI: 10.1039/C7CE01310H

an increased contribution from π···π stacking compared to other structures [Figure 7], results commensurate with the findings reported here .

Summary

In this study, we have investigated the role of C-H···π(ring) and other intermolecular interactions in seven naphthamide derivatives. The molecules under investigation were all conformationally flexible structures with lattices that were largely stabilized by contribution from dispersion energy. The π-electron regions in each of the molecules were electrostatically negative except in case of 7, where the presence of the $–NO_2$ substituent transforms the phenyl ring to positive polarity. It was clearly evident that, in addition to the molecular chains formed by strong N-H···O=C hydrogen bonds, the molecular packing was largely governed by several unique C-H···π(ring) interactions. An intramolecular hydrogen bond involving the nitro-substituent precluded the formations of a molecular chain in the case of **7**. This resulted in a markedly increased contribution to the packing from π···π stacking interactions. It also shows that the nature of substituents have a direct effect on the nature and abundance of different intermolecular interactions in a given crystal structure. Apart from the motifs formed by the N-H···O interactions, all other motifs were largely stabilized by dispersive forces especially in case of the molecular pairs generated by the C-H···π(ring) interactions. It was interesting to observe that 4 and 6 showed 3-dimensional packing isostructurality which indicate that not only the nature but also the position of the substitution can determine similarity and dissimilarity between two different structures. Analysis of the 2-dimensional Fingerprint plots revealed that C-H···π interactions were indeed the major contributors to the packing in all but one of the reported crystal structures. This study clearly illustrates that, despite the presence of a strong classical hydrogen bond, the weak C-H···π contacts were pivotal components of the crystal packing. The results further illustrate that different interactions can be tuned by performing substitution at specific positions in a molecule. Given the importance of C-H···π interactions in proteins and DNA[55-58], it will of interest in future to systematically investigate the effect of molecular environment on the propensity of these interactions in large biomolecules.

Conflicts of interest

There are no conflicts of interest to declare.

Acknowledgements

RS thanks DST-INSPIRE for a PhD fellowship. RS and DC thank IISER Bhopal for infrastructural and research facilities and SERB India for research funding. We also thank the University of Otago for purchase of the diffractometer and the Chemistry Department, University of Otago for support of the work of JS.

View Article Online
DOI: 10.1039/C7CE01310H

References

1. G. R. Desiraju, J. J. Vittal and A. Ramanan, Crystal Engineering: A Textbook, World Scientific, Singapore, 2011
2. G. R. Desiraju, *J. Am. Chem. Soc*., 2013, **135**, 9952.
3. P. Bombicz, T. Gruber, C. Fischer, E. Weber and A. Kálmán, *CrystEngComm*, 2014, **16**, 3646.
4. M. J. Turner, S. Grabowsky, D. Jayatilaka and M. A. Spackman, *J. Phys. Chem. Lett*., 2014, **5**, 4249.
5. G. R. Desiraju, *Angew. Chem. Int. Eds*., 2007, **46**, 8342.
6. M. Raynai, P. Ballester, A. Vidal-Ferran and P. W. N. M. van Leeuwen, *Chem. Soc. Rev.*, 2011, **43**, 1660.
7. H. S. Schneider, T. Schiestel and P. Zimmermann, *J. Am. Chem. Soc.*, 1992, **114**, 7698.
8. A. Tkatchenko, D. Alfé and K. S. Kim, *J. Chem. Theory Comput.*, 2012, **8**, 4317.
9. H. R. Khavasi, A. Ghanbarpour and A. A. Tehrani, *RSC Adv.*, 2016, **6**, 2422.
10. N. J. Zondlo, *Nat. Chem. Biol.*, 2010, **6**, 567.
11. K. E. Riley and P. Hobza, *Wiley Interdiscip. Rev.: Comput. Mol. Sci.*, 2011, **1**, 3.
12. M. Gurusaran, M. Shankar, R. Nagarajan, J. R. Helliwell and K. Sekar, *IUCrJ*, 2014, **1**, 74.
13. V. Ball and C. Maechling, *Int. J. Mol. Sci.*, 2009, **10**, 3283.
14. A. Nangia and G. R. Desiraju in *Design of Organic Solids*, ed. Weber, E. Springer-Verlag, Berlin, 1998.
15. K. Biradha, C.-Y. Su and J. J. Vittal, *Cryst. Growth Des.,* 2011, **11**, 875.
16. C. B. Aakeroy, N. R. Champness and C. Janiak, *CrystEngComm*, 2010, **12**, 22.
17. E. Arunan, G. R. Desiraju, R. A. Klein, J. Sadlej, S. Scheiner, I. Alkorta, D. C. Clary, R. H. Crabtree, J. J. Dannenberg, P. Hobza, H. G. Kjaergaard, A. C. Legon, B. Mennucci, D. J. Nesbitt, *Pure Appl. Chem*., 83, 1619.
18. E. Arunan, G. R. Desiraju, R. A. Klein, J. Sadlej, S. Scheiner, I. Alkorta, D. C. Clary, R. H. Crabtree, J. J. Dannenberg, P. Hobza, H. G. Kjaergaard, A. C. Legon, B. Mennucci, D. J. Nesbitt, *Pure Appl. Chem*., 83, 1637.
19. G. R. Desiraju, *Angew. Chem., Int. Ed*., 2011, 50, 52-59.
20. S. Sarkhel and G. R. Desiraju, *Proteins*, 2004, **54**, 247.
21. G. R. Desiraju, *Chem. Commun*., 2005, 2995.
22. E. Bosch, *Cryst. Growth Des*., 2010, **10**, 3808.

View Article Online
DOI: 10.1039/C7CE01310H

23. H. Haqiwara and S. Okada, *Chem. Commun*. 2016, **52**, 85.
24. L. K. Macreadie, A. J. Edwards, A. S. R. Chesman and D. R. Turner, *Aus. J. Chem.* 2014, **67**, 1829.
25. P. Panini, R. G. Gonnade and D. Chopra, *New J. Chem*., 2016, **40**, 4981.
26. P. Panini and D. Chopra, in *Hydrogen Bonded Supramolecular Structures*, ed. Z. Li and L. Wu, Lecture Notes in Chemistry, Springer-Verlag, Berlin, Heidelberg, 2015, vol. 87, pp. 37–67, ISBN: 978-3-662-45755-9.
27. R. Shukla and D. Chopra, *CrystEngComm*, 2015, **17**, 3596.
28. V. R. Hathwar, S. M. Roopan, R. Subashini, F. N. Khan and T. N. Guru Row, *J. Chem. Sci.*, 2010, **122**, 677.
29. P. P. Zhou, W. Y. Qiu, S. Liu and N. Z. Jin, *Phys. Chem. Chem. Phys.*, 2011, **13**, 7408.
30. A. Kovács and Z. Varga, *Coord. Chem. Rev.,* 2006, **250**, 710.
31. M. Nishio, *CrystEngComm,* 2004, **6**, 130.
32. M. Kumar and P. V. Balaji, *J. Mol. Model.,* 204, **20**, 2136.
33. O. Takahashi, Y. Kohno and M. Nishio, *Chem. Rev.,* 2010, **110**, 6049.
34. M. Nishio, *Phys. Chem. Chem. Phys*., 2011, **13**, 13873.
35. T. Steiner, *Angew. Chem. Int. Ed.,* 2002, **41**, 48.
36. S. Tsuzuki, K. Honda, T. Uchimaru, M. Mikami and K. Tanabe, *J.Am. Chem. Soc.*, 2000, **122**, 3746.
37. Y. Umezawa, S. Tsuboyama, K. Honda, J. Uzawa and M. Nishio, *Bull. Chem. Soc. Jpn.*, 1998, **71**, 1207.
38. A. Gil, V. Branchadell and M. J. Calhorda, *RSC Adv.,* 2016, **6**, 85891.
39. S. Tsuzuki, K. Honda, T. Uchimaru, M. Mikami and K. Tanabe, *J. Phys. Chem. A*, 1999, **103**, 8265.
40. S. Tsuzuki, K. Honda, A. Fujii, T. Uchimaru and M. Mikami, *Phys. Chem. Chem. Phys.*, 2008, **10**, 2860.
41. S. Tsuzuki, A. Fujii, *Phys. Chem. Chem. Phys.*, 2008, **10**, 2584.
42. A. Stone, *J. Chem. Phys. Lett.*, 1993, **211**, 101.
43. O. Takahashi, Y. Kohno and M. Nishio, *New J. Chem.,* 2013, **37**, 2082.
44. O. Takahashi, Y. Kohno, K. Ueda and M. Nishio, *New J. Chem.,* 2013, **37**, 843.
45. M. Nishio, Y. Umezawa, J. Fantini, M. S. Weiss and P. Chakrabarti, *Phys. Chem. Chem. Phys.,* 2014, **16**, 12648.
46. C. J. McAdam, S. A. Cameron, L. R. Hanton, A. R. Manning, S. C. Moratti and J. Simpson, CrystEngComm, 2012, 14, 4369.

View Article Online
DOI: 10.1039/C7CE01310H

47. R. Carrillo, M. López-Rodríguez, V. S. Martin and T. Martín, *Angew. Chem. Int. Ed.*, 2009, **48**, 7803.
48. Y. Kobayashi, T. Kurasawa, K. Kinbara and K. Saigo, *J. Org. Chem.,* 2004, **69**, 7436.
49. Y. Ryan, P. W. Peterson, C. M. Hadad and J. D. Badjic, *Chem. Commun.,* 2014, **50**, 9086.
50. P. Sozzani, A. Comotti, S. Braco and R. Simonutti, *Chem. Commun.,* 2004, 768..
51. H. Brunner, T. Tsuno and M. Bodensteiner, Organometallics, 2014, **33**, 2257.
52. E. C. Constable, K. Harris, C. E. Housecroft, M. Neuburger and J. A. Zampese, *CrystEngComm*, 2010, **12**, 2949.
53. C. D. Scala, H. Chahinian, N. Yahi, N. Garmy and J. Fantini, *Biochemistry*, 2014, **53**, 4489.
54. A. K. Pandey, K. M. Thomas, C. R. Forbes and N. J. Zondlo, *Biochemistry*, 2014, **53**, 5307.
55. M. Kufmann, M. Gisler and C. J. Leumann, Angew. *Chem. Int. Ed.*, 2009, **48**, 3810.
56. S. M. Butterfield, M. M. Sweeney and M. L. Waters, *J. Org. Chem.*, 2005, **70**, 1105.
57. M. Kumar and P. V. Balaji, *J. Mol. Model*, 2014, **20**, 2136.
58. M. Brandl, M. S. Weiss, A. Jabs, J. Sühnel, R. Hilgenfeld, *J. Mol. Biol*., 2001, **307**, 357.
59. N. Mohan, K. P. Vijayalakshmi, N. Koga and C. H. Suresh, *J. Comp. Chem*., 2010, **31**, 2874.
60. S. Tsuzuki, K. Honda, T. Uchimaru, M. Mikami and K. Tanabe, *J. Am. Chem. Soc*., 2000, **122**, 3746.
61. J. C. Harmandge, M.M. Weiss, J. Germain, A. J. Polverino, G. Borg, J. Bready, D. Chen, D. Choquette, A. Coxon, T. DeMelfi, L. DiPietro, N. Doerr, J. Estrada, J. Flynn, R. F. Graceffa, S. P. Harriman, S. Kaufman, D. S. La, A. Long, M.W. Martin, S. Neervannan, V. F. Patel, M. Potashman, K. Regal, P. M. Roveto, M. L. Schrag, C. Starnes, A. Tasker, Y. Teffera, L. Wang, R. D. White, D. A. Whittington and R. Zanon, *J. Med. Chem.,* 2008, **51**, 1649.
62. P. Carato, A. Graulich, N. Jensen, B. L. Roth, J.-F. Liégeois, *Bioorg. Med. Chem. Lett.,* 2007, **17**, 1570.
63. M. Résimont, J.-F. Liégeois, *Bioorg. Med. Chem. Lett.,* 2010, **20**, 5199.
64. Harper, T. Jenkins-West, P. C. Levesque, D. E. Normandin, A. D. Russell, R. P. Serafino, M. A. Smith and N. J. Lodge, *J. Med. Chem.,* 2001, **44***,* 3764.
65. Y. Laras, C. Garino, J. Dessolin, C. Weck,V. Moret, A. Rolland and J. L. Kraus JL. *J Enzyme Inhib Med Chem.* 2009 **24**, 181.
66. A. Saeed, M. F. Erben and M. Bolte, *J. Org. Chem.,* 2012, **77**, 4688.

View Article Online
DOI: 10.1039/C7CE01310H

67. Bruker *APEX2*, *SAINT* and *SADABS*. Bruker AXS Inc., Madison, Wisconsin, USA, 2011.
68. G. M. Sheldrick, *Acta Crystallogr.,*2008, A**64**, 112.
69. K. A. Hunter and J. Simpson, *TITAN2000*. University of Otago, New Zealand, 1999.
70. C. F. Macrae, I. J. Bruno, J. A. Chisholm, P, R. Edgington, P. McCabe, E. Pidcock, L. Rodriguez-Monge, R. Taylor, J. van de Streek and P. A. Wood, *J. Appl. Cryst.*, 2008, **41**, 466.
71. A. L. Spek, *Acta Crystallogr.,* 2009. **D65**, 148.
72. L. J. Farrugia, *J. Appl. Cryst.*, 2012, **45**, 849.
73. A. Gavezzotti, *New J. Chem.,* 2011, **35**, 1360.
74. A. Gavezzotti, *J. Phys. Chem. B*, 2003, **107**, 2344.
75. A. Gavezzotti, *J. Phys. Chem. B*, 2002, **106**, 4145.
76. P. Panini and D. Chopra, in Hydrogen Bonded Supramolecular Structures, ed. Z. Li and L. Wu, Lecture Notes in Chemistry, Springer-Verlag, Berlin, Heidelberg, 2015, vol. 87, pp. 37–67, ISBN: 978-3-662-45755-9.
77. R. Shukla and D. Chopra, *CrystEngComm,* 2015, **17**, 3596.
78. M. J. Turner, J. J. McKinnon, S. K. Wolff, D. J. Grimwood, P. R. Spackman, D. Jayatilaka and M. A. Spackman, CrystalExplorer17 (2017). University of Western Australia. http://hirshfeldsurface.net.
79. M. A. Spackman and J. J. McKinnon, *CrystEngComm*, 2002, **4**, 378.
80. J. J. McKinnon, D. Jayatilaka and M. A. Spackman*, Chem. Commun*., 2007, 3814.
81. T. Gelbrich and M. B. Hursthouse, *CrystEngComm*, 2006, **8**, 448.
82. F. P. A. Fabbiani, B. Dittrich, A. J. Florence, T. Gelbrich,M. B. Hursthouse, W. F. Kuhs, N. Shankland and H. Sowa, *CrystEngComm*, 2009, **11**, 1396.
83. C. R. Groom, I. J. Bruno, M. P. Lightfoot and S. C. Ward, *Acta Cryst.,* 2016, **B72**, 171.
84. S. Karthikeyan, V. Ramanathan and B. K. Mishra, *J. Phys. Chem. A*, 2013, **117**, 6687.
85. G. Cavallo, P. Metrangolo, R. Milani, T. Pilati, A. Priimagi, G. Resnati and G. Terraneo, *Chem. Rev.,* 2016, **116**, 2478.
86. A. Bondi, *J. Phys. Chem.,* 1964, **68**, 441.
87. H. R. Khavasi, A. Ghanbarpour and A. A. Tehrani, *CrystEngComm*, 2014, **16**, 749.
88. Z. A. De los Santos, R. Ding and C. Wolf, *Org. Bimol. Chem.,* 2016, **14**, 1934.